010266-1-T

10266-1-T = RL-2197

THE UNIVERSITY OF MICHIGAN

COLLEGE OF ENGINEERING

DEPARTMENT OF ELECTRICAL AND COMPUTER ENGINEERING

Radiation Laboratory

A SPACE DEPLOYED HOLOGRAM ANTENNA

PRELIMINARY DESIGN

by

Joseph E. Ferris

August 1972

2216 Space Research Building
2455 Hayward Street

Ann Arbor, Michigan
48105

TABLE OF CONTENTS

INTRODUCTION

The purpose of this report is to consider the feasibility of developing an antenna for use with a hologram radar system to be operable from a space vehicle. Chapter I discusses the preliminary requirements of the antenna as they pertain to the space environment.

Chapter II notes some of the electro-mechanical problems that will require attention. Typical problems noted are cabling requirements, array surface flatness, and the need for additional elements. A challenging problem associated with a large space deployed antenna is the prevention of warping in the antenna surface or the provision of some means for electronically correcting for surface warpage. One method for electronically correcting for antenna warpage is suggested.

In Chapter III we discuss several antenna space considerations under two major headings: 1) Environmental Factors, and 2) Spacecraft Parameters. Under Environmental Factors the following items are addressed: atmospheric drag, thermal effects, and material mass loss and surface deterioration. Studies to date show that atmospheric drag is not of critical concern for spacecraft orbiting at altitudes 200 miles above the earth. To minimize thermal effects, efforts are made 1) to employ thoroughly stable material, 2) to employ material possessing high thermal conductivity properties, and 3) to employ structural designs that are readily analyzed for thermal deformations. Past studies have shown that the effects of mass loss and surface deterioration are not critical. However, these studies do recommend that the use of cadmium in the space environment be avoided.

In considering the spacecraft parameters, one must be aware of the space limitations within the spacecraft as well as weight limitations associated with the booster vehicle. Therefore, consideration may have to be given to the use of light-weight space deployable antennas. It is typical for spacecraft to have some finite motion along the pitch, roll and yaw axis, and these variations must be taken into account in the antenna design. Consideration is given to the feasibility of deploying the antenna outside the spacecraft as well as to fabricate it as a part of the space vehicle.

In Chapter IV we discuss the present state-of-the-art of space deployed antennas. Some new materials being used to minimize thermal effects are noted as are the techniques employed in the fabrication of large antenna structures.

In Chapter V a hologram antenna design is discussed and design curves are presented. A major portion of the discussion is concerned with the across track antenna design. In Chapter I it is suggested that it may be desirable to employ a $1.4(10)^4\lambda$ aperture across track. In this discussion we attempt to show that the hologram antenna is effectively a high speed scanned phased array. Therefore, care must be exercized to ensure that grating lobes do not occur within the region from which imaging data is to be collected. The curves presented are to aid in this area of the antenna design. A short discussion is presented for the along track design. This aspect of the antenna is relatively straightforward because of the relatively small aperture needed along track.

Because of the large number of array elements required employing a conventional filled array we have concluded a short exploratory study of array thinning techniques. The results of this study are noted in Chapter VI. From this investigation it appears promising to employ thinning techniques, however, it is felt that future microwave hologram studies should include an optical simulation of thinned arrays.

Chapter VII discusses a tentative side-looking high-resolution radar antenna design. The recommended antenna is a parabolic cylinder (10 feet long by 0.63 feet wide). The reflector is to be fed by a line source feed (an edge-shunt waveguide slot array).

Various antenna configurations that were considered for both the hologram array and the side-looking radar antenna are briefly discussed in Chapter VIII.

1.0 Antenna Requirements

In a recent memo (R. Larson, 1971) antenna element dimensions were specified based on several system parameters. Figure 1 shows the physical aperture along with the pertinent dimensions.

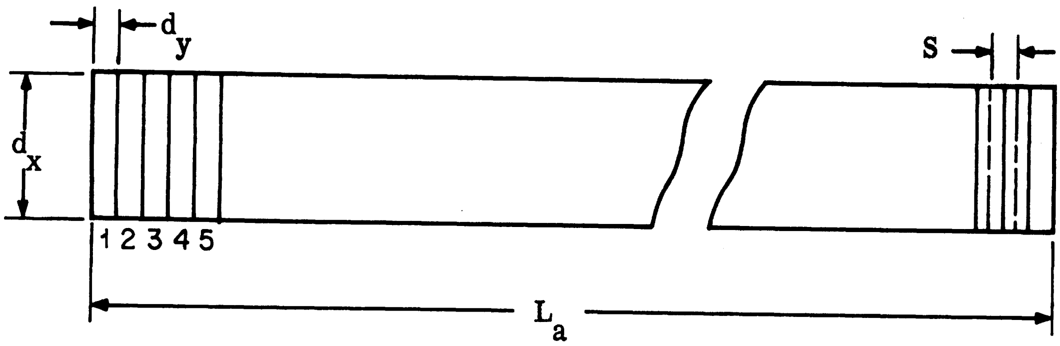

FIG. 1: Physical Aperture of Antenna.

The system parameters of Larson's memo are:

Satellite Alt (r) = 235 nautical miles (nm),
Satellite Velocity (v) = 25,000 ft/sec.,
Number of antenna elements (N) = 1200,
Cross track resolutions (ρy) = 100 feet,
Along track resolutions (ρx) = 100 feet.

Based on these parameters, it was shown that the required dimensions (d_x and d_y) for each element of the array and the overall array length (L_a) should be as shown in Table I.

TABLE I

Normalized Antenna Dimension

$$d_y = 6\lambda$$
$$d_x = 60\lambda$$
$$L_a = 1.4(10)^4\lambda$$

Combining the above normalized dimensions with wavelengths associated with frequencies of 1.0, 10.0 and 100.0 GHz, we obtain the physical dimensions of Table II.

TABLE II

Physical Dimensions of Antenna versus Frequency

Frequency (GHz)	d_y (feet)	d_x (feet)	L_a (feet)
1.0	6.0	60.0	$1.4(10)^4$
10.0	0.6	6.0	$1.4(10)^3$
100.0	0.06	0.6	$1.4(10)^2$

2.0 Antenna Electro-Mechanical Considerations

Below we shall discuss some of the pertinent factors associated with the microwave hologram antenna as they may pertain to the space environment.

First, let us note that the antenna to be used is in a sense, a phased array, operating passively. However, it is not terminated in the conventional manner where some form of RF feed structure is employed leading to a single RF output. Instead each element of the array is terminated by a separate receiver, i.e., there are N elements and N receivers. The N outputs from the receivers contain both amplitude and phase information which is recorded on some form of memory device such as film or magnetic tape. These individual data are then processed to form the desired imagery. To insure that high quality imagery is obtained, the antenna design must have radiation pattern characteristics (in both planes) that properly illuminate the area on the ground to be mapped. To simplify the data processing, it is desirable for the radiation patterns of the N elements to be identical. In addition, the physical location of the phase centers associated with each of the N elements relative to a reference point must be known, e.g., it is desirable for the phase centers of the N elements to be located on a straight line and in the same plane.

To achieve identical antenna patterns it is desirable to employ a simple antenna structure such that mechanical tolerances (typically $< 0.1\lambda$) can be readily held so that it will be feasible to fabricate the required several hundred elements employing state-of-the-art techniques. To further insure that the radiation patterns are identical, it may be necessary to employ a few dummy elements at each end of the array. During the development of a previous hologram antenna array (Zimmerman 1967), it was shown that the radiation patterns of the end elements differed from those in the center (this array consisted of 100 elements see Figure 2). To minimize this effect, additional dummy elements were placed at each end of the array. This hologram antenna array was fabricated with the phase centers on a common line and in the same plane. This was easily feasible since the aperture of the physical array was relatively small, i.e., approximately 50λ long and 9λ wide and the design was for operation at K_u band (17 GHz).

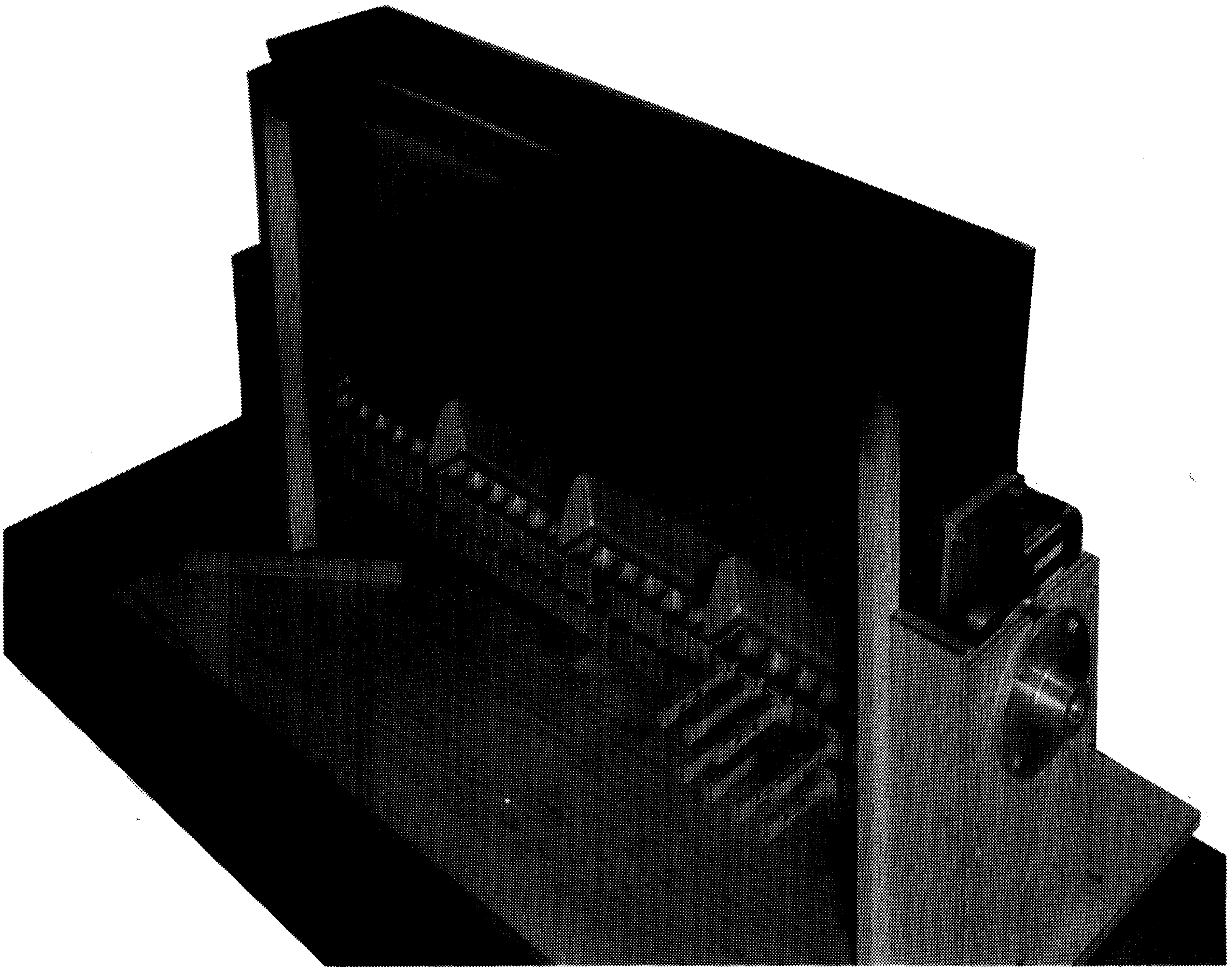

FIG. 2: Final Configuration of 100 Active Element Hologram Array.

For the present system the objective is for an aperture dimension approximately $1.4(10)^4\lambda$ long by 60λ wide. Because of the length of the array, it may not be feasible to fabricate the array to maintain the phase centers of the identical elements on a common line and in the same plane because of elasticity of the metal. Typically, in conventional phased arrays considerable effort is expended to locate the phase centers of individual elements with $\lambda/16$ relative to a straight line of a plane surface. This suggests that the aperture of an E-band array should be flat over a 140 foot by 7.2 inch aperture surface to within 0.008 of an inch. It is recognized that this degree of flatness is unrealistic for an unsupported array. However, it may be feasible to provide for corrections electronically to cause the array to appear to be flat to the degree necessary.

Since data collected by each element of the hologram antenna is processed individually it is possible to compensate for the improper location of the phase centers associated with the individual elements of the array. A method might be provided to measure the location of the phase centers associated with each of the array elements (relative to a reference point). This information could be used to adjust the relative phase of the individual elements during data collection or data processing.

A method suggested for making the phase center measurement in the space environment requires that a reference source be located in the vicinity of the space borne array and that two sets of data be recorded. This reference source may be either an active or passive device and its position known $(\pm \lambda/8)$ with respect to a point on or near the array surface. Assume that the reference source is an active device, e.g., a small horn, whose phase center is accurately known with respect to a reference point on the array. The phase center locations of the hologram array elements would be determined as follows.

Initially the hologram array elements must be phase aligned on the ground to ensure that a flat phase front is received by the hologram antenna. This step is necessary regardless of the size of the array. The phase alignment is accomplished by adjusting the relative phase associated with each of the N elements to be $0 \pm \lambda/16$ relative to one of the elements within the array. After this initial phase alignment has been completed, the reference source (small horn above) would be excited and the first set of data recorded as follows.

The RF energy radiated by the reference source would be collected by each of the hologram array elements. This data would be processed by the hologram radar and recorded for future reference. Because of the nature of the hologram radar the data recorded would contain the reference phase information that is associated with a flat array. The second set of phase data would be collected after the antenna has been assembled in space. For this set of data, the reference source would be positioned in the same location as before relative to the hologram array. RF energy radiated by the reference source would be collected and recorded for each of the N elements. The phase change associated with each of the N elements would be determined by comparing the two sets of data. The necessary correction in phase would be made by making the necessary phase adjustment associated with each of the array elements.

3.0 Antenna-Space Considerations

To aid in determining how large an antenna may be employed with a hologram radar, consideration must be given to at least the following two areas:

1) Environmental factors,
2) Spacecraft parameters.

Associated with each of these major areas are sub-areas which will be discussed briefly.

3.1 Environmental Factors

In a previous report (Lockheed 1958) several environmental factors were noted as possible sources of concern to the design of unfurlable antennas for space applications. For the present microwave hologram radar study, consideration must be given to several of these factors although an unfurlable antenna is not envisioned. The method of deploying the hologram antenna may range from a self-erectable rigid structure to a rigid structure erected by astronauts in space. Since the writing of the above report several space programs have been carried out by NASA which have demonstrated the successful deployment and operation of antennas in deep space, e.g., the Surveyor and Manned Space programs. However, the antenna required for the hologram radar will be considerably larger than those employed in the above programs (see Table II). At least three of the environmental factors noted by Lockheed must be considered in the design of the hologram antenna:

1) Atmospheric drag,
2) Thermal effects,
3) Material mass loss and surface deterioration.

3.1.1 Atmospheric Drag

The aerodynamic drag (B) on a body is directly proportional to its area and inversely proportional to its mass as follows.

$$B = \frac{C_D A}{2M} \tag{1}$$

where C_D = drag coefficient (refs 2, 3, 4),

A = projected satellite area upon which C_D is based,

M = mass of the satellite.

It has been shown (Breakwell et al 1958) that the lifetime of a satellite is dependent upon its orbital altitude and eccentricity in addition to the projection of its area on a plane perpendicular to the direction of its velocity vector relative to the atmosphere. Therefore, a satellite with furled antennas will have a longer lifetime than the same satellite would have with unfurled antennas as shown below.

Simplifying Breakwell and Koehler's formulation for the number of orbital revolution to

$$N = \frac{K}{B} \tag{2}$$

where

K = constant (Breakwell and Koehler),

B = see eq. 1.

To show how the lifetime of a satellite is reduced when the antenna is unfurled, employ the following equation for the lifetimes fo the satellite with the antenna furled (sub 1) and unfurled (sub 2).

$$N_1 = \frac{K}{B_1} \quad , \tag{3}$$

and

$$N_2 = \frac{K}{B_2} \quad . \tag{4}$$

Assuming the satellites have identical masses (M) and drag coefficients (C_D) it may be shown (combining Eq. 1, 3 and 4) that the lifetime of the satellite with the antenna unfurled is

$$N_2 = \frac{N_1 A_1}{A_2} \quad . \tag{5}$$

From Eq.(5) if the area of the unfurled antenna, in the plane perpendicular to the satellite velocity vector, is significantly larger than the area of the satellite with the antenna furled, in the same plane, the lifetime of the satellite will be reduced significantly (see Fig. 3-4). It is conceivable that the lifetime of the satellite with a large unfurled antenna could be increased through the use of an active propulsion system. However, this would then reduce the space available for laboratory equipment in the spacecraft. Therefore, it is desirable for the deployed hologram antenna to be physically as small as possible so as not to impair the performance of either the satellite or the space available for laboratory experiments. Therefore, to minimize the atmospheric drag while maximizing radar resolution it would be desirable to employ an antenna which operates at the highest frequency feasible (Table II).

3.1.2 Thermal Effects

Satellite antennas such as the hologram antenna intended for use in outer space will be exposed to severe temperature fluctuations ranging from -200° to +300°F. Exposure of the antennas to these temperature variations may lead to mechanical and/or electrical failure. However, if care is exercized in the initial design and fabrication of the antenna, destructive thermal effects may be avoided.

For the hologram antenna it is conceivable that millimeter wavelengths may be employed. For this reason it will be necessary to maintain very close mechanical tolerances (.001 inches) not only in the fabrication of the individual elements but also during their exposure to the space environment. The Lockheed report (1958) discusses temperature effects in considerable detail and that information is, therefore, omitted here. However, we shall note some of the techniques to be considered to minimize temperature effects.

To minimize thermal exposure effects use should be made of metal alloys that are temperature stable and have a high rate of thermal conductivity for those components whose dimensional tolerances are critical. For those components whose dimensional tolerances are less critical, the metal surfaces might be oxidized to improve the thermal conductivity. To prevent warpage attention should be given to the use of thin wall metals where practical to minimize thermal gradients.

As a part of the antenna design a thermal analysis of the antenna must be performed. This analysis will aid in arriving at a design with a minimum of antenna distortion and it will provide considerable insight as to time intervals during which the antenna can and cannot be used. As the antenna design and thermal analysis progresses considerable knowledge will be gained so the system engineer can be provided information as to the manner in which the antenna will physically behave in space. With this information the systems engineer may be able to compensate for antenna deformations through data processing. It is understood that engineers at Convair, San Diego (1969), and Lockheed, Sunnyvale (1970) have made thermal analyses for space deployed antennas currently under study at these facilities.

One of the more difficult thermal problems exist when a portion of the antenna is in its own shadow or in the shadow of the spacecraft thus causing a large temperature gradient to exist on the antenna surface. Temperature gradients tend to cause structures to become distorted. Titanium alloys (0.16 pounds per cubic inch) tend to possess reasonably good dimensional stability but these alloys exhibit poor thermal conductivity. Invar is a heavy material (0.3 pounds per cubic inch) and tend to possess reasonably good dimensional stability and have a high thermal conductivity property. A new graphite/epoxy alloy has recently been receiving some attention because of its low weight (comparable to titanium) and its excellent dimensional stability and high thermal conductivity. A recent brochure (Convair 1971) illustrates the RMS deviation of a 70 foot reflector as a function of orbit time. The data presented in the above report assumes that the antenna is constructed from either a titanium or a graphite epoxy alloy such that they have respectively a maximum RMS deviation of 0.130 and 0.040 inches when the solar flux (from the sun) illuminates the reflector parallel to its aperture surface. Therefore, any advanced study for the hologram antenna should include further investigation into the use of these graphite/epoxy alloys. A possible source of information would be Convair (San Diego) Division of General Dynamics.

3.1.3 Material Mass Loss and Surface Deterioration

Because of the combination of high temperature and low pressure, metals such as magnesium and cadmium are extremely susceptible to damage in the space environment (i.e. material depletion). Use of these metals should be minimal and then only in those areas where mechanical tolerances are not important. A third space hazard is due to the action of meteorites (large and small). Micrometeoroids may be very damaging to the antenna since they could, if they strike the antenna, dent or even puncture the antenna to the extent of destroying the radiation and/or electrical characteristics of the antenna. Materials used in the construction of the antenna must be able to withstand both of these hostile environmental effects of outer space.

3.2 Spacecraft Parameters

To aid in the design of the hologram antenna certain spacecraft parameters must be taken into consideration. Initially a knowledge of space available for storing the antenna while in transit from the earth to its space location is required. At present it is felt the antenna should be constructed in a modular-rigid form rather than to employ unfurlable antenna techniques. Since the size of the antenna is inversely proportional to the RF frequency (see Table II) the choice of frequency is also important. Tentatively 200 cu.ft. would be required for the storage of an E-band antenna. Another spacecraft parameter of interest is its weight-carrying capacity. As a rough estimate the weight of a 1000 element E-band antenna fabricated from a titanium alloy would be approximately 1000 pounds. Lower frequency antennas would no doubt be heavier since their weight is proportional to their volume.

The orbiting altitude has a definite influence on cross track aperture size of the antenna. Larson (1971) shows that the cross track aperture dimension is directly proportional to the orbiting altitude of the space vehicle, e.g. an E-band antenna orbiting at an altitude of 235 nautical miles has an L_a = 140 feet and for a 100 nautical mile altitude has an L_a = 60 feet.

The method of assembling and fastening the antenna to the spacecraft must also be considered in determining the maximum size of the antenna. There are two possible approaches: 1) the antenna is assembled outside the space vehicle after orbital altitude is reached, and 2) the antenna is installed as a part of the vehicle during the pre-launch preparation.

In the event the antenna is assembled in space, consideration must be given both to the method of attachment to the spacecraft and additional structural members that would be required. Presently it is envisioned that a space erected antenna would be supported at its center of gravity (probably at its geometrical center) with the ends of the antenna unsupported. It is understood that space vehicles have a tendency to have a small oscillatory roll about the vehicle axis, e.g. the Skylab vehicle has an oscillatory roll of approximately $\pm 2^{\circ}$ at a rate of $.05^{\circ}$/sec. If we assume that the acceleration forces associated with this roll are equally applied to all parts of the vehicle including extended members (such as the antenna) the antenna would not experience any bending. However, in the event it is necessary to energize the roll thrusters occasionally to correct for excessive rolling of the vehicle a space-erected antenna would experience some finite bending, thus introducing phase errors over the aperture surface. This would then necessitate recalibrating the antenna (as noted above in 2.0) to ensure that quality imagery is obtained.

Provision must also be provided for transferring data collected by each of the N elements and their receivers to the data recording media. The most practical means for transferring data is through cables. To provide some insight as to the complexity of this problem it is conceivable that there may be from 300 - 1000 antenna elements and receivers from which data must be recorded. Assuming the antenna is erected outside the spacecraft and the recording media and receiver power sources inside the spacecraft, it is apparent that a considerable amount of interconnecting cabling would be required. These interconnecting cables would no doubt further complicate the hologram system because of their vast number as well as the fact that they would be exposed to the hostile environment of outer space.

The principal advantage for employing a space-erected antenna is that there are no physical space limitations associated with the size of the antenna. However, when one considers the problems associated with rigidizing, calibrating and protecting the antenna from the hostile environment of outer space, one sees many system limitations associated with employing a space-erected antenna. In addition consideration must be given to weight and the complications associated with the large number of interconnecting cables, since this might further limit the effectiveness of the overall space borne experiment. Therefore, at this time it is difficult to specify how large an antenna could be erected in space for use with a hologram system.

An alternate technique would be to design the antenna for installation in the airframe of the spacecraft. One disadvantage of this technique would be that the maximum size of the antenna would be limited by the spacecraft dimensions, e.g., the length L_a of the hologram array would be limited to approximately 30 feet when installed in a Skylab vehicle. In the event it is feasible to install the antenna in the spacecraft some knowledge about the amount of bending and twisting which takes place within the structure of the spacecraft will be required. In the event such movement is found to be excessive, consideration will have to be given to methods of isolating the antenna structure from the spacecraft. It is understood that a spacecraft is typically flown such that its largest dimension is parallel to its velocity vector. This orientation is believed to be chosen to minimize the atmospheric drag on the spacecraft. In the event a hologram antenna is installed along the long dimension of the spacecraft, it would be necessary for this dimension to be oriented perpendicular to the spacecraft velocity vector during those periods mapping data is recorded. If the craft is orbiting at a low altitude ($\leq$ 100 miles) its lifetime will be drastically reduced (see Figures 3 and 4) when its long dimension is oriented perpendicular to the velocity vector.

Placing the antenna within the spacecraft would help to protect it from damage by meteorites. Also, it may be possible to isolate the antenna from the variable thermal environment of space, e.g. the antenna termperature could be maintained at a relatively constant low (-200^{o}F) temperature. Another alternative would be to install a radome over the antenna to facilitate maintaining the temperature within the antenna compartment within some finite controlled limits. With the antenna mounted within the confines of the spacecraft the problems associated with the interconnecting cables would be minimal.

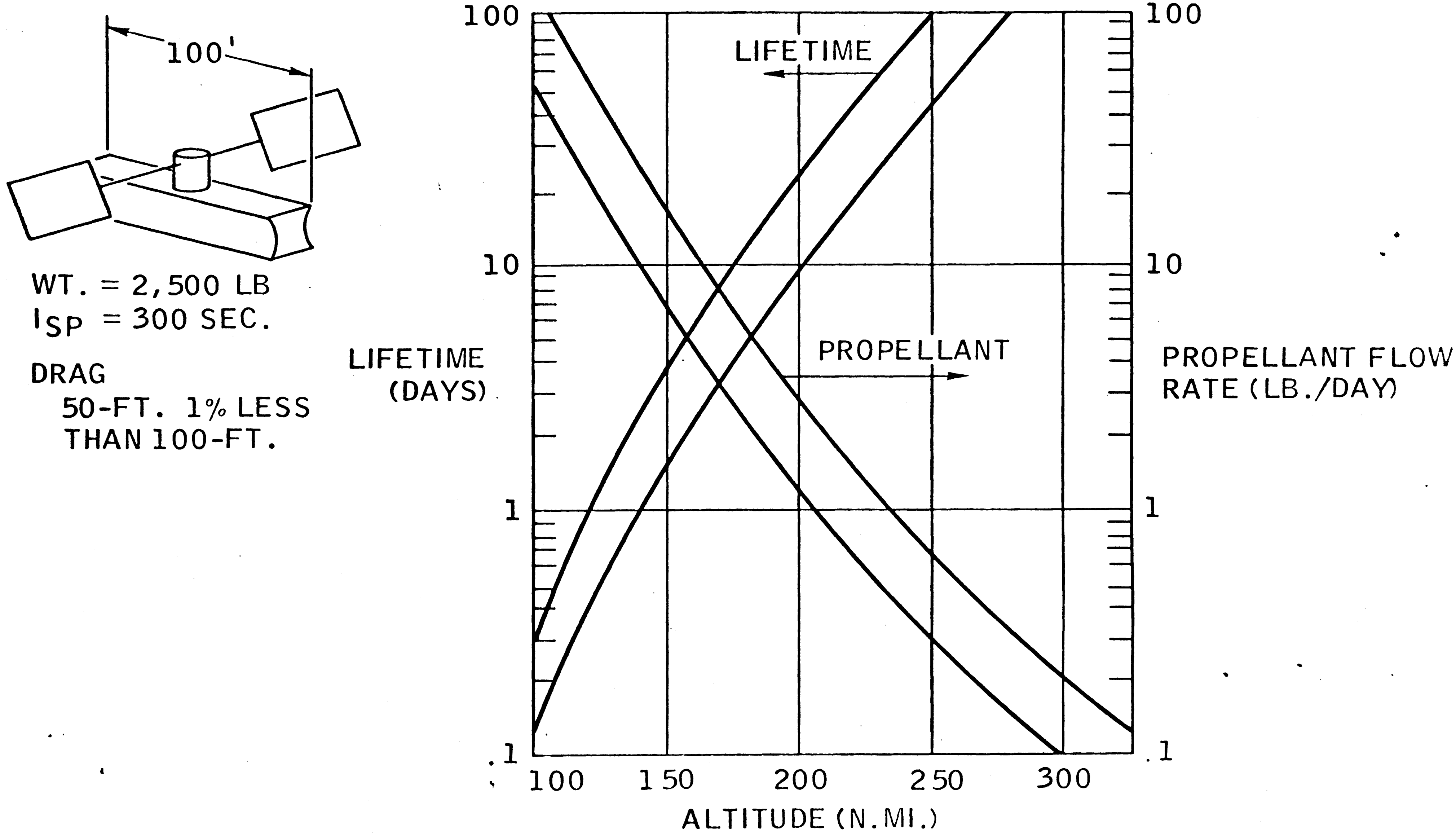

FIG. 3: Side Looking Radar Space Flight Consideration.

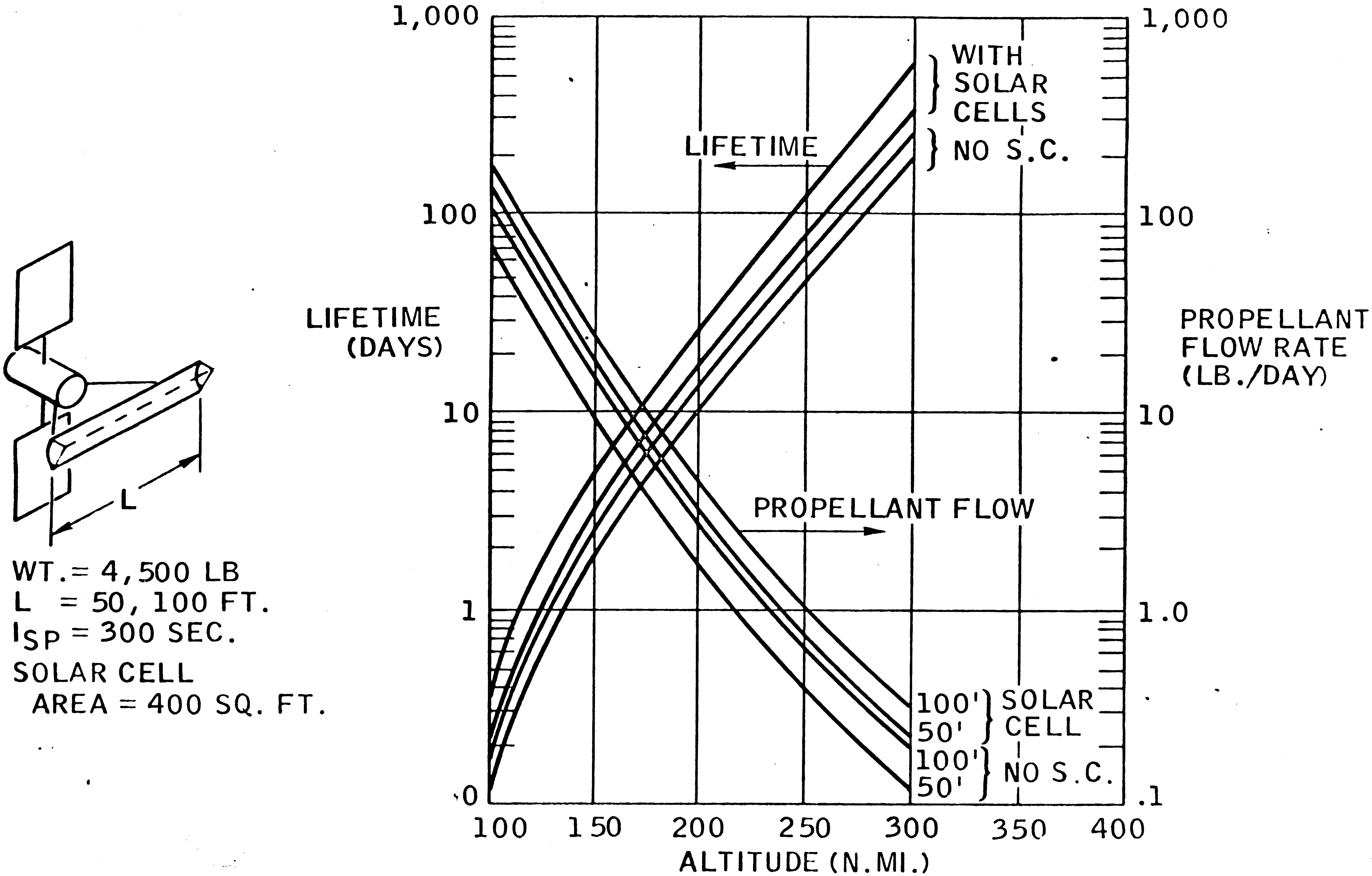

FIG. 4: Hologram Radar Space Flight Considerations.

4.0 1971 Space Deployed Antennas

Large space erectable antennas now being conceived and fabricated employ relatively simple structures. Typically these are reflector antennas that range in size from a few feet to 100 feet in diameter. The upper frequency of operation has been about 10 GHz. The majority of these large antennas employ a metalized mesh for the reflecting surface because of its light weight and optical transparency (to minimize temperature gradients). Some have felt that these conductive meshes could be used at higher frequencies but at present there is no data in the open literature to substantiate these feelings. Some smaller antennas (1.5 foot diameter) have been fabricated using a graphite epoxy alloy (Dietrich, 1970) that operate at a frequency of 60 GHz.

Designers of space borne antennas state that the principal problem to be faced is that of minimizing thermal effects. One of the more challenging thermal problems associated with parabolic reflectors results when the sun shines edgewise on the dish. To cope with the thermal problem antenna designers employ relatively simple configurations so that the antenna can be readily and accurately analyzed for thermal deformaties.

In the design of large space borne antennas, care must be exercized to ensure that the deployed antenna does not significantly shorten the spacecraft lifetime. This is particularly true for those spacecrafts that orbit ≤ 100 miles above the earth. This problem becomes less serious for spacecraft orbiting about 200 miles (Figures 3 and 4).

The present state-of-the-art for the fabrication of space borne antennas suggests that for a design goal an E-band antenna 100 - 150 feet long may be feasible by 1976. To accomplish this it will be necessary to establish a preliminary antenna design and begin to subject it to thermal analyses within the next year. The antenna design should be kept simple and employ a minimum number of flexible joints. This will aid in obtaining a more accurate thermal analysis of the antenna. Since it is important for the hologram antenna to possess a flat phase front across its aperture some means must be provided for periodically measuring this property of the antenna in space. Two techniques that have been suggested would either employ a microwave signal to measure the actual phase distortion or a laser beam to measure the physical distortion of the antenna. The need for this requirement requires further study and if required a particular technique must be developed and implemented.

5.0 Hologram Antenna Design

A tentative antenna design as conceived would consist of approximately 2800 elements. Each element would be an asymetrically fed parabola (hog-horn configuration) having a dual polarized feed at the focus of the parabola. The aperture of the hog-horn would be $d_y \times d_x$ and the dual polarized feed is envisioned to be a dual polarized E-band slot array approximately d_λ long. Individual elements would be arrayed into subarrays and subjected to thermal analysis to optimize their length. A typical element is shown in Fig. 5.

It is envisioned that the parabolic surface would be molded from a graphite epoxy alloy and the side walls would be fabricated from a conductive mesh. The edge supports will be flexible members to facilitiate folding the antenna for storage during flight and to minimize thermal gradients during deployment. If feasible these flexible members and the dual polarized feed will be fabricated from a graphite epoxy alloy, to further reduce thermal deformation of the antenna. It is anticipated that the subarrays can be manufactured in 10 foot lengths such that 14 would be required to deploy a 140 foot long E-band dual polarized hologram antenna array. To support the array some form of backup structure (trusses) will be required. It is envisioned that the antenna could be an unfurlable or telescopic structure.

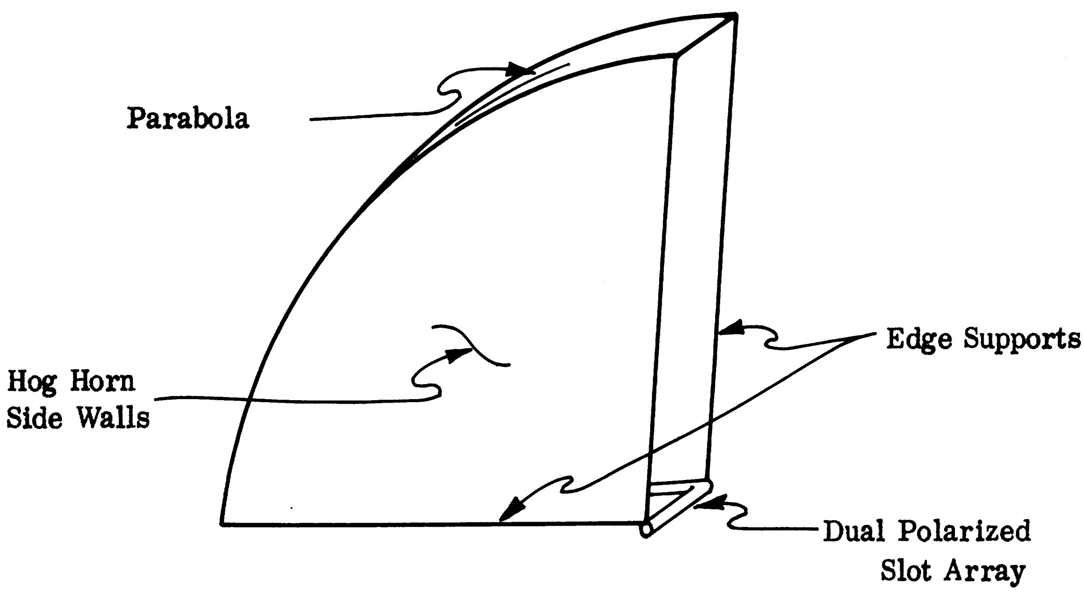

FIG. 5: Hologram Array Element (Hog-Horn).

Based on the above tentative design the following analysis is made to aid in establishing $d_y \times d_x$. We shall employ the coordinate system of Fig. 6. The antenna aperture (A) lies in the x-y plane and radiates energy in the +z direction. The polarization shall be referred to as either $E\theta$ or $E\phi$, depending on whether the electric field E, associated with the radiated energy, is parallel to unit vectors $\hat{\theta}$ or $\hat{\phi}$ respectively of Fig. 6.

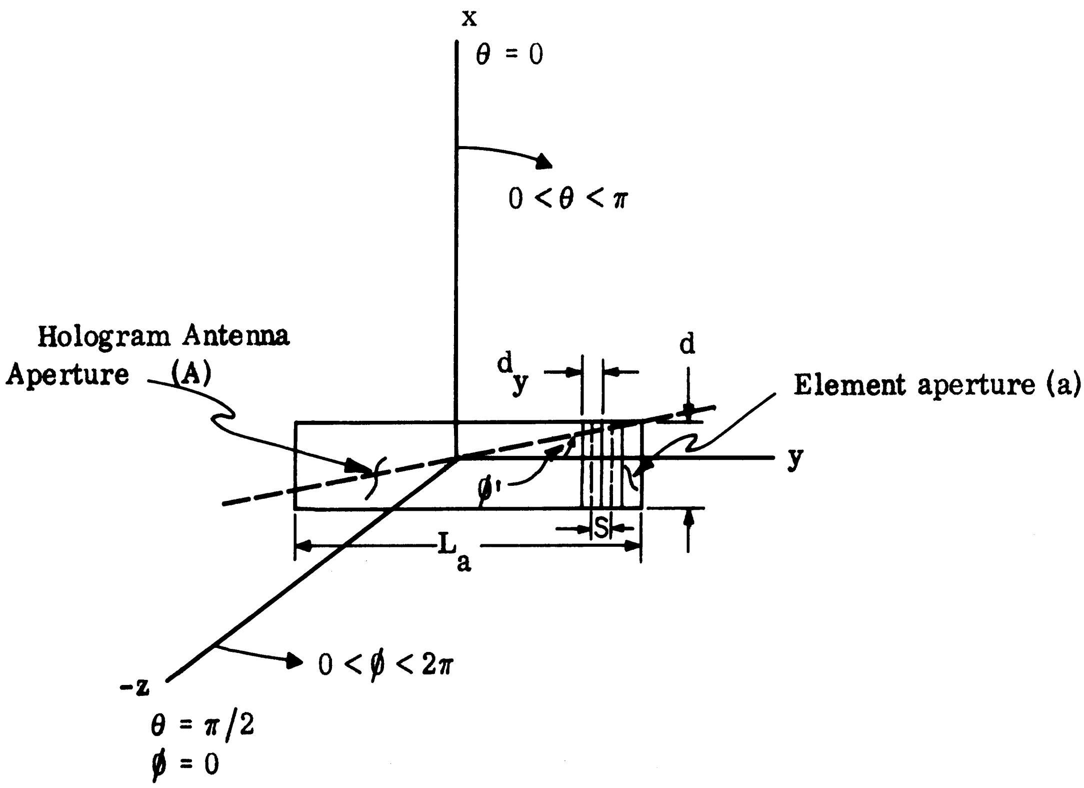

FIG. 6: Hologram Antenna Coordinate System.

5.1 Across Track Antenna Design

Initially we are interested in determining the radiation characteristics of the hologram array in the y - z plane. Therefore, we require some knowledge of the pattern associated with the individual element apertures (a) and the array factor associated with the N element array in the y - z plane.

The radiation pattern in the y - z plane of Fig. 1 for the hologram antenna may be expressed as:

$$E_+ = 20\log\left\{\frac{S}{L_a}\,\frac{\sin\frac{L_a\pi}{\lambda}(\sin\phi-\phi')}{\sin\frac{S\pi}{\lambda}(\sin\phi-\phi')}\right\} + 20\log\frac{\sin\frac{\pi d_y\phi}{\lambda}}{\frac{\pi d_y\phi}{\lambda}}\,, \qquad (5)$$

where

S = element spacing,

L_a = total length of array,

ϕ = angle of interest across track,

ϕ' = beam steer angle,

d_y = element width across track,

λ = wavelength.

The first term of Eq. (5) is the array factor of the antenna and the second term is the assumed radiation pattern for the individual elements of the array. The element pattern has been plotted in a normalized form in Fig. 7. The width of the ground swath (y) illuminated (between the half power points of the element pattern factor) by the individual elements as a function of the element width (d_y), altitude (r) of the antenna and the wavelength (λ) of the energy transmitted is obtained using the following expression which has been extrapolated from Eq. (5),

$$(x, y) = \frac{r\,(0.88)\,\lambda}{d(x, y)} \text{ n. miles} \qquad (6)$$

the nomograph shown in Fig. 8 has been plotted to show how the sizes of the ground swath varies as a function of the above three variables. For the purposes of this nomograph the ground swath is plotted in nautical miles. As is apparent from Eq. (6) the ground swath is directly proportional to the spacecraft altitude and λ of the signal transmitted and inversely proportional to the element width. To illustrate the use of the nomograph let us assume an element width $d_y(\lambda)$ of 5λ and an altitude r of 235 n. miles the ground swath width (y) from which data is to be collected will be approximately 44 nautical miles. The size of the ground swath determines the window size from which imagery data is collected.

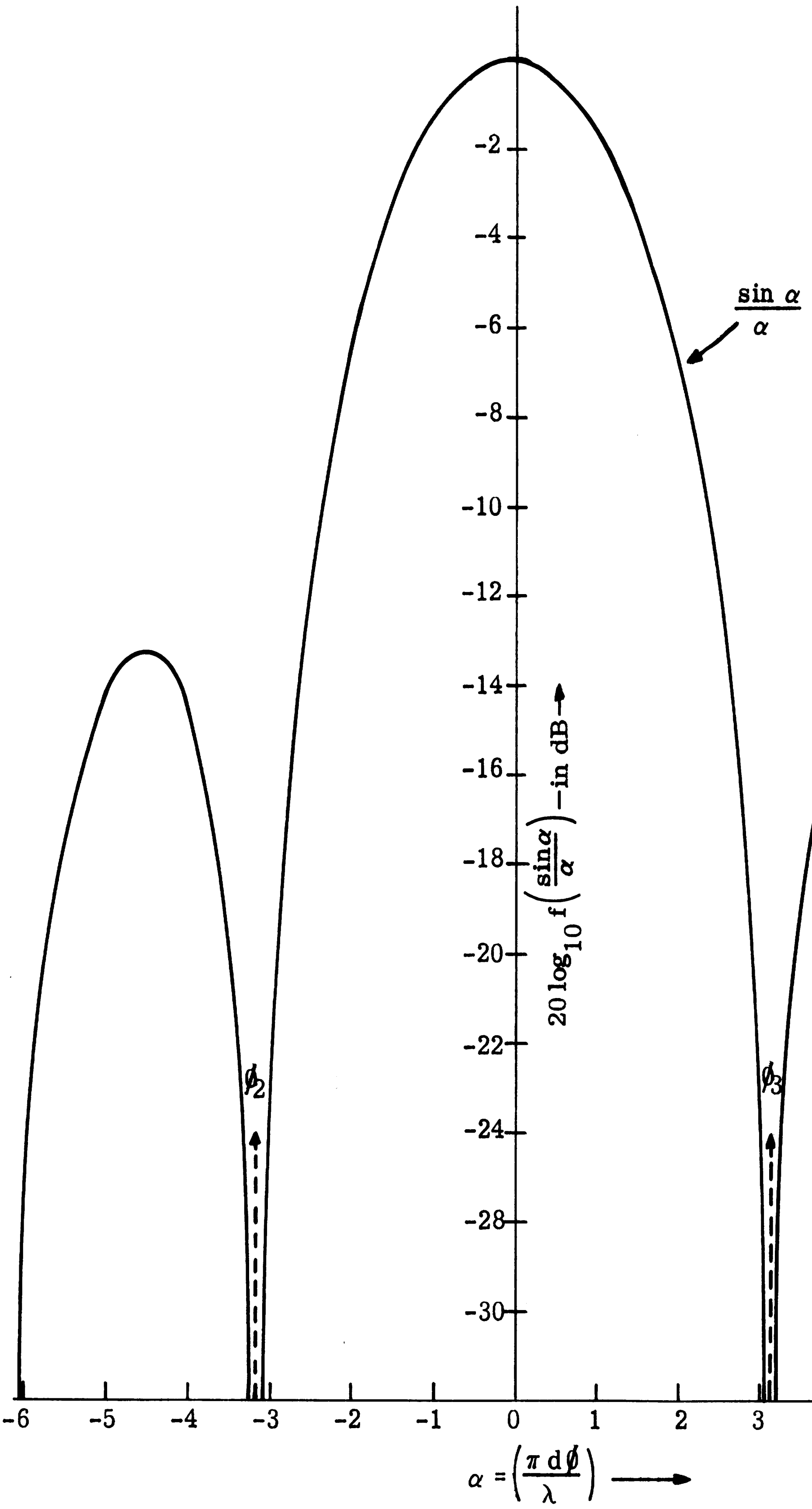

FIG. 7: Element Pattern Factor $\frac{\sin \alpha}{\alpha}$.

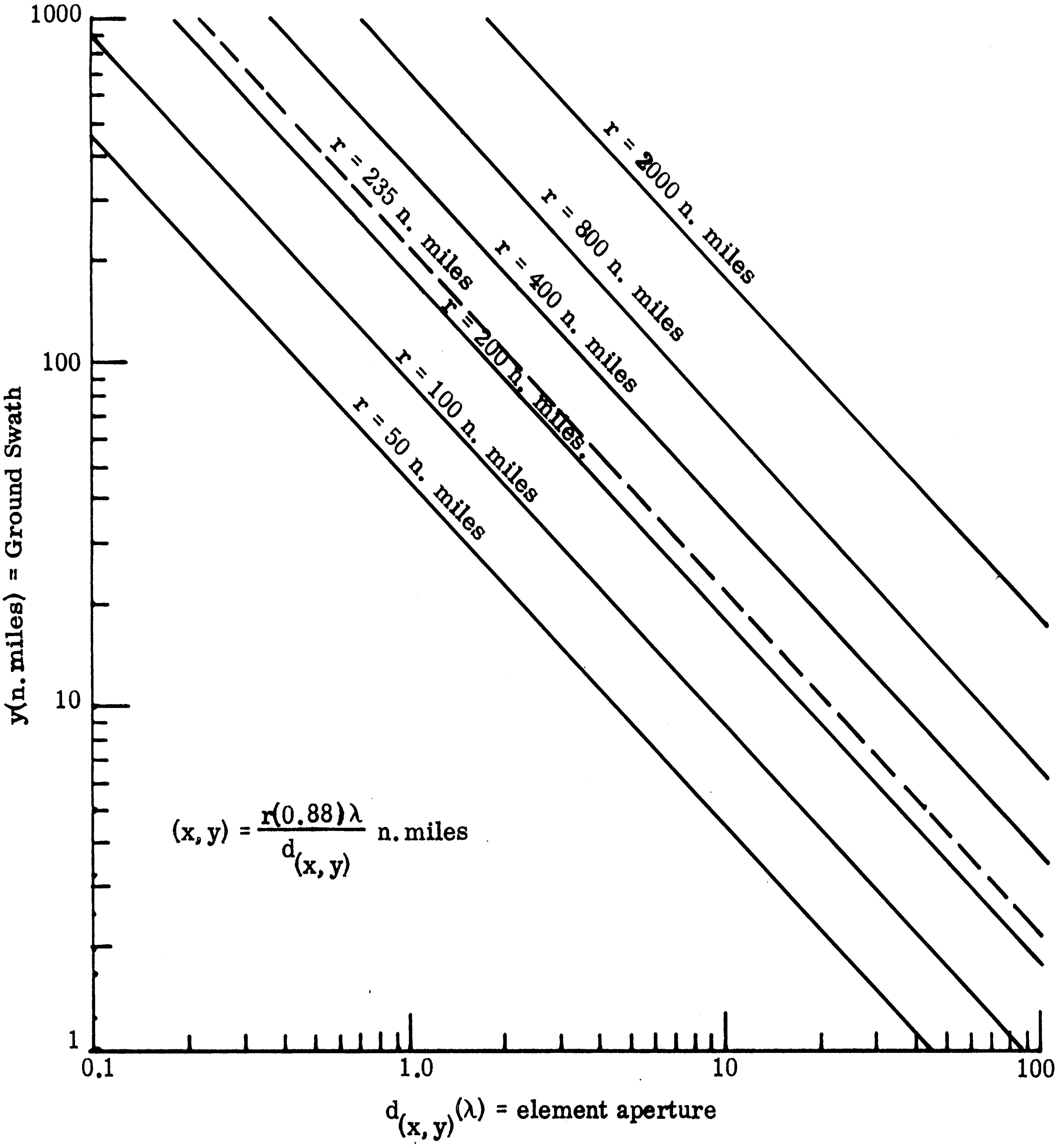

FIG. 8: Ground Swath Width.

We have noted that each element of the hologram array will collect data from a large ground swath (y). The amplitude and phase of the data collected by each element will differ because of differences associated with each element's look-at angle. However, when the data is properly processed imagery will be obtained whose resolution (ρ) is proportional to the half power beamwidth associated with the total across track array length (L_a).

$$\rho_{(y)} = \frac{(r)\, 5340\, \lambda}{L_a} \quad , \tag{7}$$

where (see Fig. 9),

r = n. miles,

L_a = feet,

ρ = feet.

Effectively it may be shown that the array major lobe is being scanned through a finite angle (ϕ') either side of broadside. Therefore, it may be concluded that the across track imagery is related to the amount of beam steer required to ensure that the ground swath of interest is adequately illuminated.

It has been noted that the width of the ground swath (across track) illuminated by the antenna is a function of the width of the array elements across track. In addition, it has been noted that the imagery resolution ρ_y (across track) is related to the array length (L_a) across track. Referring to Fig. 8 it may be seen that an element width (d_y) of 5.4λ or less is required to illuminate an across track (y) ground swath of 40 n. miles from an antenna at an altitude of 235 n. miles. Referring to Fig. 6 it may be seen that the spacing (S) between adjacent elements within the array is related to the element width (d_y) and is typically larger. To scan the total array pattern over this ground swath (y) width a scan angle (beam steer = ϕ') of plus and minus 5 degrees would be required. It can be shown by

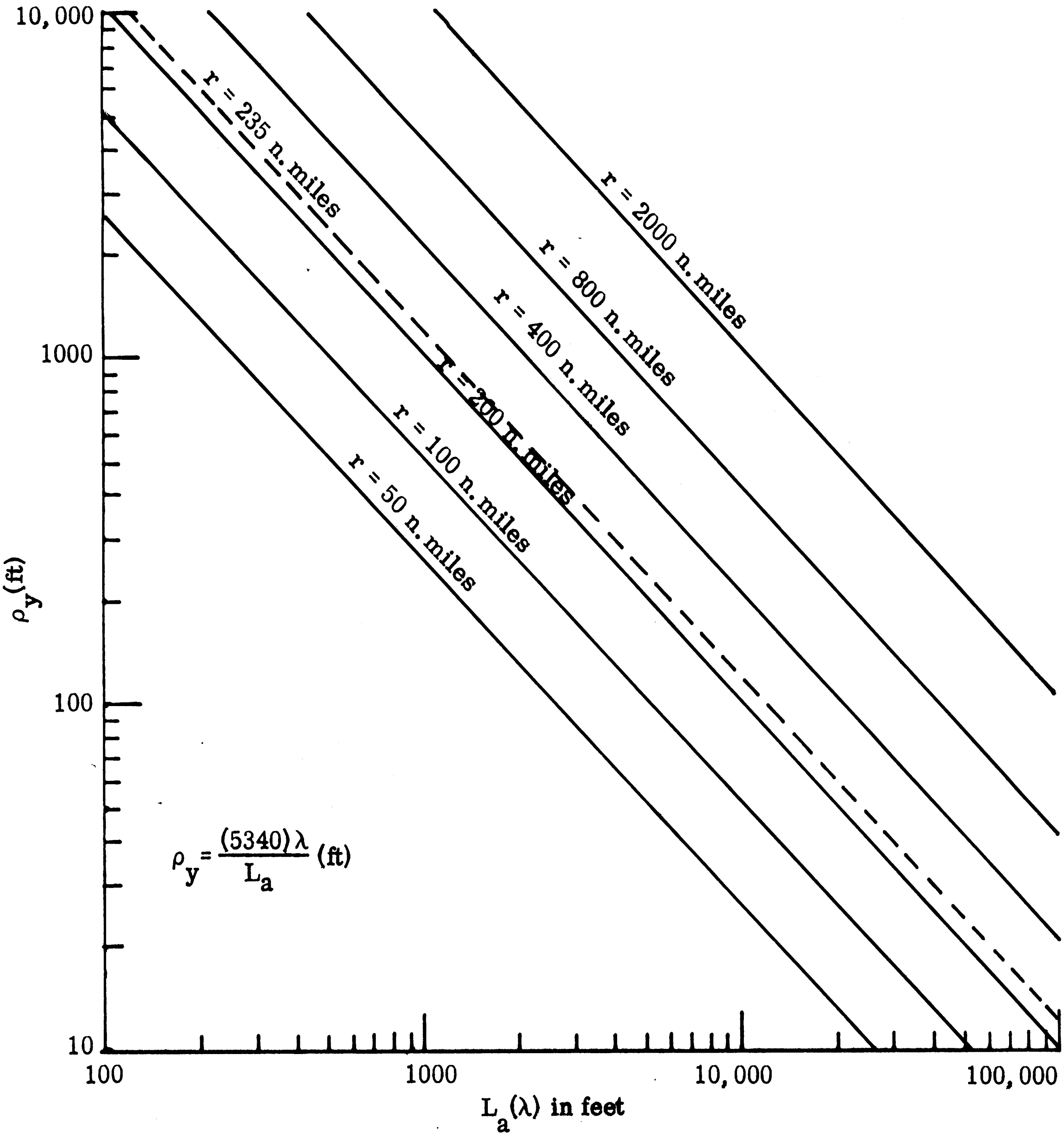

FIG. 9: Across Track Resolution.

inspection of Eq. (5) that when beam steering an array of elements spaced greater than $\lambda/2$ apart high intensity side lobes (grating lobes) comparable in energy content to the major lobe of interest are generated. To ensure that unambiguous imagery is obtained care must be exercized to avoid the generation of grating lobes that illuminate the ground swath (y) of interest.

The angular position of the grating lobes may be obtained from an inspection of the denominator of the first term of Eq. (5). This can be done by setting the argument of the denominator equal to $n\pi$ and evaluating the resulting equation as a function of element spacing (S) and beam steer angle (ϕ'). Figure 10 is a plot of the above expression for $n=1$, $S=3$, 4, 5 and 6λ, and $0 \leq \phi' \leq 9^{o}$. From an inspection of Fig. 10 it is noted that two grating lobes appear and are designated as ϕ_2 and ϕ_3 (see Fig. 11). We note from Fig. 10 that as the beam is steered from $\phi = 0$ to ϕ' that the grating lobes located at ϕ_2 and ϕ_3 move respectively toward and away from $\phi = 0$. To ensure that unambiguous imagery is achievable for a 40 n. mile ground swath ϕ_2 and ϕ_3 must be outside of the -5^{o} to $+5^{o}$ limits. Referring to Fig. 10 we see that the spacing (S) should be approximately 5λ to ensure that the above restriction is satisfied. To provide some insight as to the manner in which the magnitude of the major lobe and grating lobes 2 and 3 vary relative to the major lobe maximum ($\phi' = 0$) as a function of beam steer Figs. 12 and 13 are shown. It is seen that the amplitude of the above lobes are a function of the element width (d_y) and the element spacing (S).

To illustrate the use of Figs. 10, 12 and 13, assume an element spacing (S) of 5λ and element width (d_y) of 4λ. We have used different values for S and d_y to account for the possibility of employing a conducting spacer between elements. Referring to Figure 10 and assuming a beam steer ϕ' of +4 degrees, we see that grating lobes ϕ_2 and ϕ_3 will occur

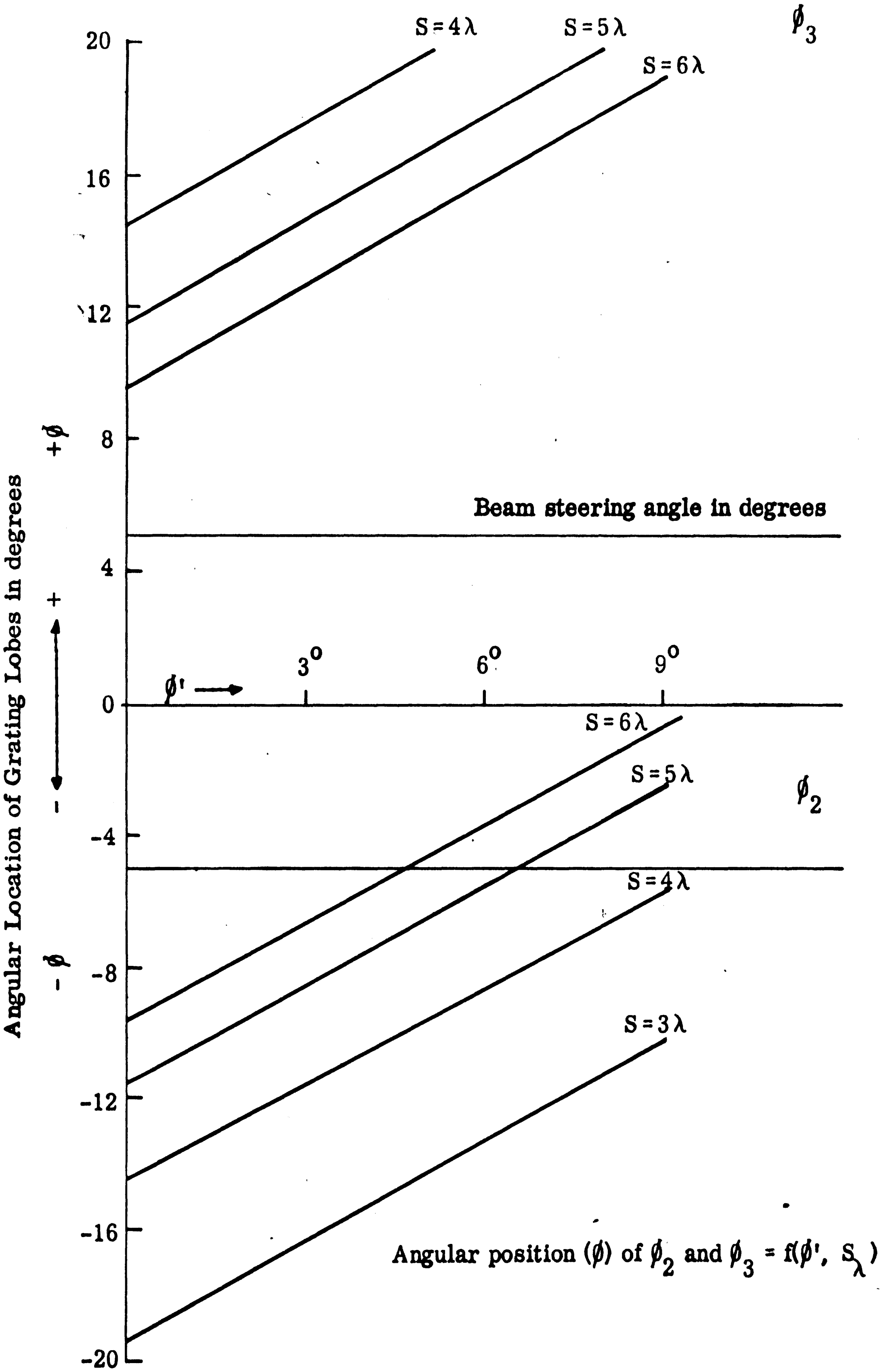

FIG. 10: Angular Location of Grating Lobes

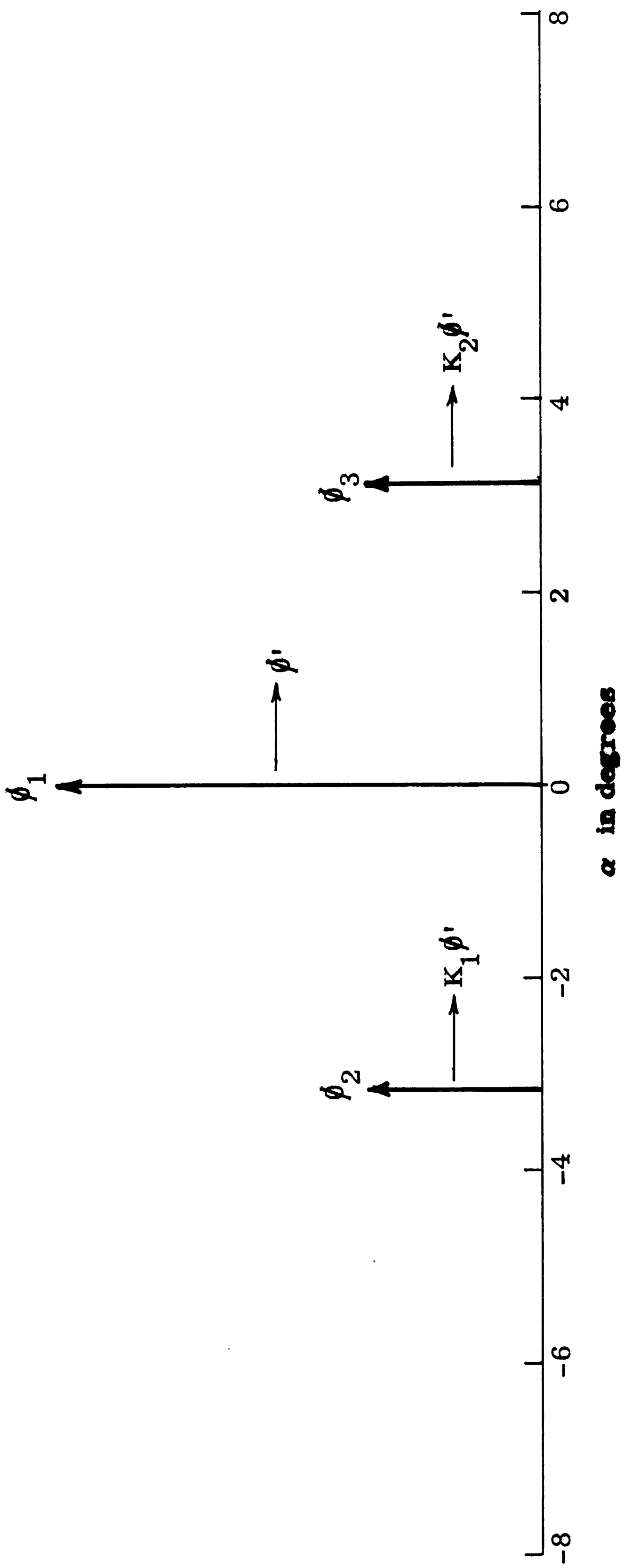

FIG. 11: Grating Lobe Position.

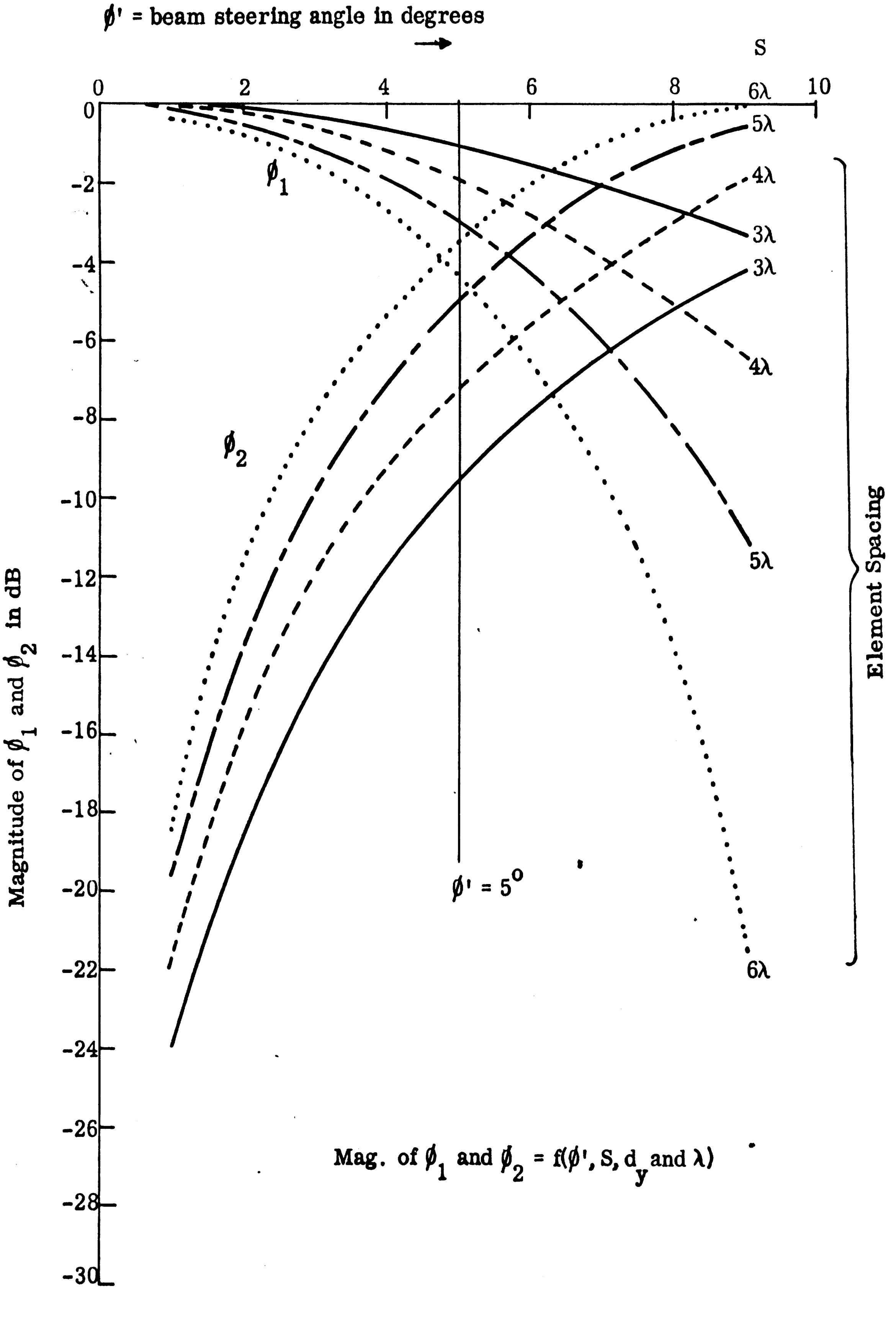

FIG. 12: Amplitude of Grating Lobe (ϕ_2) and Major Lobe (ϕ_1)

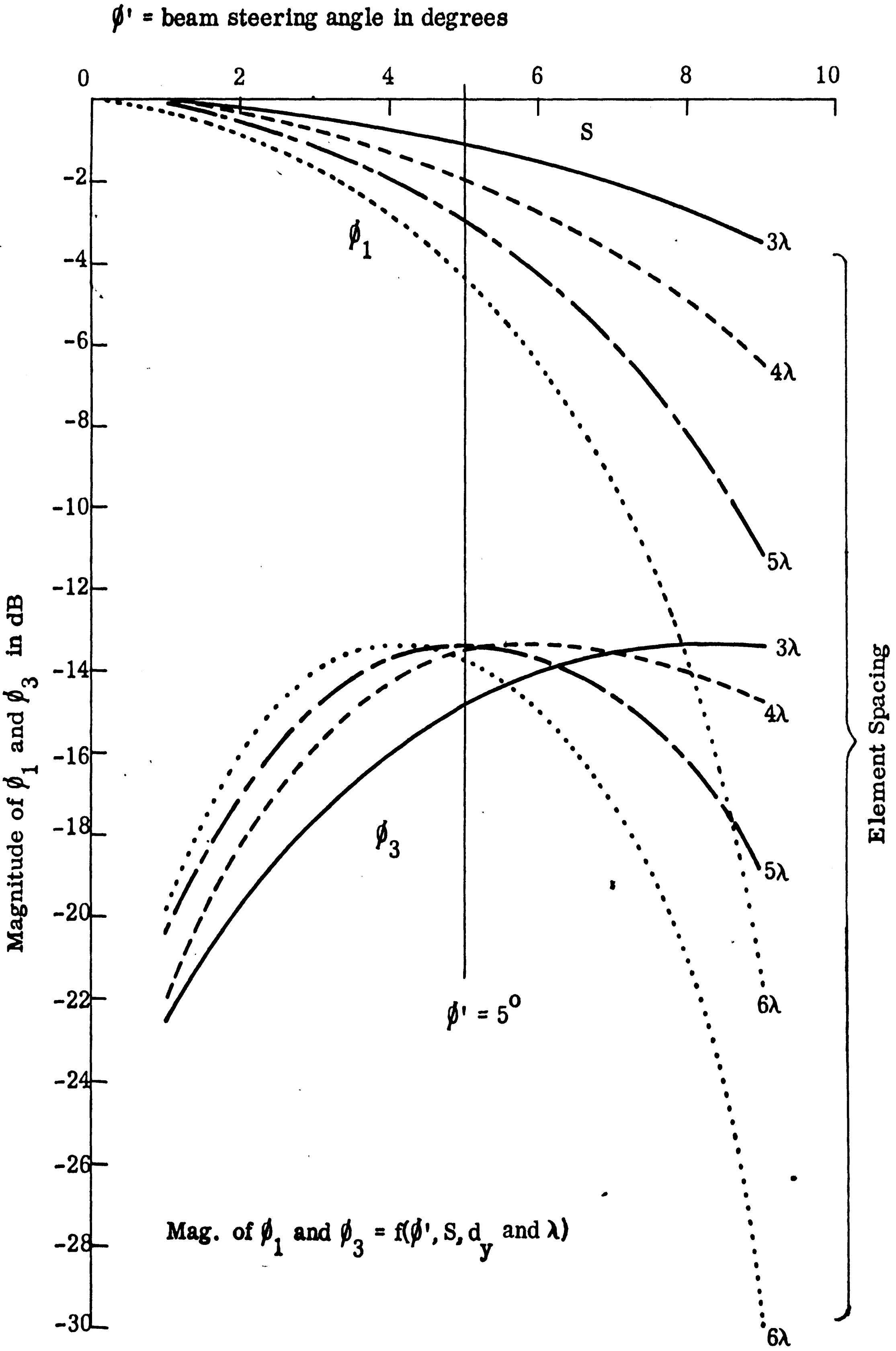

FIG. 13: Amplitude of Grating Lobe (ϕ_3) and Major Lobe (ϕ_1)

respectively at ϕ = -6.5 and 15.6 degrees. It should be noted that the main lobe of the array will occur at $\phi = \phi' = +4$ degrees. The magnitude of ϕ_2 and ϕ_3 lobes (Fig. 12 and 13) for $\phi' = 4^o$ will be the maximum at the above angles and will be -7.8dB and -14.2dB respectively with respect to the major lobe maximum assuming no beam steer ($\phi' = 0$). The major lobe (ϕ_1) will be -1.3dB with respect to the major lobe maximum assuming no beam steer ($\phi' = 0$). Information on the maximum number of elements N (spaced S apart) required in an array L_a long is given in Figure 14.

5.2 Along Track Antenna Design

To achieve the desired along track resolution (ρ_x) Synthetic Aperture Radar (SAR) techniques will be employed. Harger (1970) shows that by employing SAR techniques a resolution along track equal to 1/2 the antenna's along track aperture size d_x could be achieved for the hologram system.

$$\rho_x = \frac{d_x}{2} . \qquad (8)$$

Employing this expression, it is apparent that ρ_x is directly proportional to the physical antenna aperture size. Therefore to achieve 30 meters along track. resolution (ρ_x) an aperture size (d_x) of 60 meters should be used. It should be noted here that expression (7) assumes that all data captured within the 3dB beamwidth of the antenna (associated with the physical antenna aperture (d_x)) is recorded and processed. This then places a severe requirement on the stability of the vehicle transporting the antenna. For the subject effort it would be necessary to specify that the pitch, roll and yaw associated with the spacecraft be zero. This is not felt to be realistic since there will be experiments on board the spacecraft that will have moving parts associated with them such that some spacecraft motion in pitch, roll and yaw will be experienced and will have to be corrected for periodically. Although it is conceivable that some means could be provided to control the position of the antenna to ensure that it would always be properly pointed toward the area being mapped, it is felt that the required instrumentation would add significantly to the weight and complexity of the system. As a consequence we shall consider a less efficient but a more realistic approach.

Harger (op cit) further shows that the resolution (ρ) may be expressed as follows:

$$\rho = 0.88 \frac{\lambda R}{2 v T} \tag{9}$$

where

R = short range,

v = vehicle velocity,

T = time during which data is collected

λ = wavelength of radar carrier frequency.

It is also shown that the length of time (T) the scattered signal is collected by the antenna is determined effectively by the pattern (along track for the subject case) of the physical antenna. It has been assumed that the antenna has an aperture of length (d_x) uniformly illuminated such that it has a 3dB beamwidth (θ_3)

$$\theta_3 = \frac{0.88 \lambda}{d_x} \quad . \tag{10}$$

For simplicity the pattern is assumed to have unit amplitude within (θ_3) and zero outside such that the maximum time (T) the scatterer is illuminated and data recorded is (assuming $\theta_3 < 10$ degrees).

$$T = \frac{\theta_3 R}{v} \tag{11a}$$

or

$$T = \frac{0.88\lambda\ R}{d_x\, v} \quad . \tag{11b}$$

Referring back to Eq. (8) we see that ρ is inversely proportional to T such that

$$\infty > \rho_x > \frac{d_x}{2} \quad , \tag{12a}$$

for

$$0 > T > \frac{\theta_3 R}{v} \quad . \tag{12b}$$

Therefore, we note that there is a range of T (Eq. 11b) for which data may be collected and recorded. However, for $T < \frac{\theta_3 R}{v}$ we see from Eq. (8) that the resolution (ρ) will be less than $d_x/2$ such that the system is less efficient than that noted in Eq. (7).

Because of the probability of spacecraft motion (roll, pitch and yaw) we propose to employ an antenna having a smaller aperture antenna along track than is dictated by Eq. (7). Through the use of the smaller aperture, the area illuminated will be greater than the area mapped to compensate for spacecraft motion. To ensure that the desired resolution is achieved the period (T) during which data is recorded will be appropriately limited in accordance with Eq. (8).

Typically it is assumed that spacecraft motion may be limited in roll, pitch and yaw to less than 1.0 degree. Therefore, to ensure that targets of interest are adequately illuminated an along track half power beamwidth (θ_x) of 1 degree is recommended. Assuming uniform illumination for the aperture (d_x) we may calculate the aperture size (d_x) from

$$\frac{d_x}{\lambda} = \frac{.88}{\theta_x} \tag{13}$$

where θ_x is measured in radians. Therefore, to achieve a 1.0 degree (0.0174 radian) 3dB beamwidth the antenna aperture along track should be approximately 51λ wide.

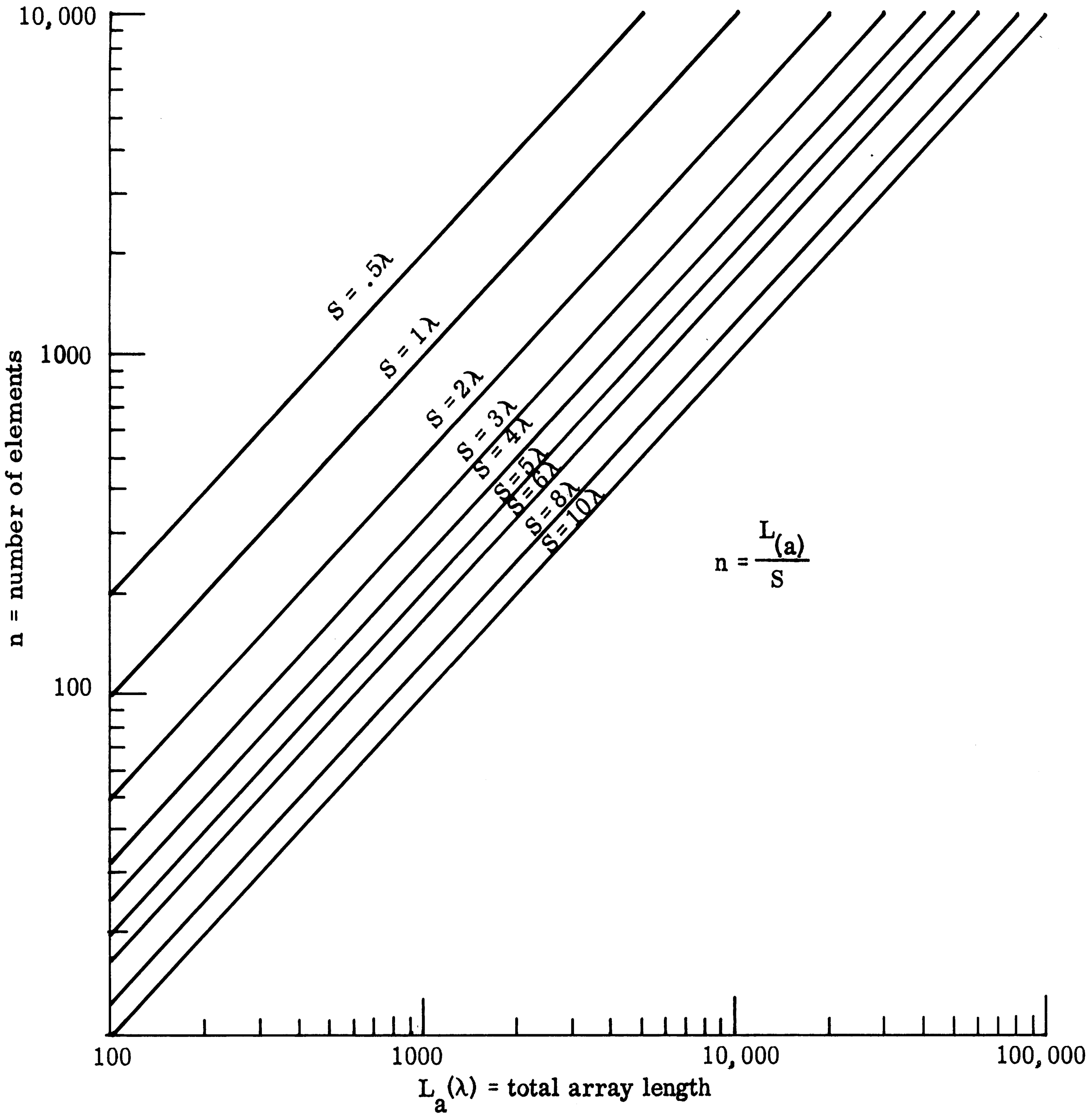

FIG. 14: Maximum Number of Elements Required.

6.0 Hologram Array, Element Thinning

To achieve 100 foot cross track resolution from an E-band (100 GHz) microwave radar system, section 5 shows that a 2800 element filled array (elements placed side by side) would be required. This would necessitate the use of an equal number of receivers and a considerable amount of cabling thus contributing significantly to the weight of the system. To minimize system weight, an exploratory study was conducted to determine the minimum number of array elements required. Skolnik (1969) and others have shown that arrays of large numbers of elements can be thinned significantly (elements of a filled array removed) and achieve respectable far field radiation patterns. These investigators have compared radiation pattern data from filled arrays (arrays having $\lambda/2$ elements spaced $\simeq \lambda/2$ apart) and thinned arrays (arrays having $\lambda/2$ elements, spaced $\geq \lambda/2$ apart). Depending upon the antenna application they have shown that array thinning factors of 50 percent - 90 percent can be employed.

Thinning techniques are numerous, however, as a consequence of past experience, it was decided that statistical thinning as discussed by Skolnik (op cit) be employed for the purposes for the study.

To satisfy the requirement of the hologram system, the elements of the array must be 5λ wide and the array length must be $1.4(10)^4\lambda$ long. Therefore, a filled array would require 2800 elements. For the purposes of our initial study we thinned an E-band (100 GHz) array by 50 percent such that there would be 1400 active elements. Later the array was thinned to 87, 92.8 and 96.4 percent. In addition we investigated the feasibility of employing 75 percent thinning for X (10 GHz) and K_a (35 GHz) band arrays, each 100 feet long.

Initially the E-band array was divided into 28 sections of 100 elements each. Each of the 28 subsections consisted of both active and inactive elements. The active elements for each case noted above were distributed such that more were located in the center of the array than near the ends and were distributed to simulate a cosine function along the length of the array (with cos 0 at the center of the array). A typical distribution employed for the E-band array is shown in Table III. It should be noted that the active elements were all assumed to be excited equally such that active elements were assigned an excitation of "1" and inactive element an excitation of "0". Since each element was 5λ wide it was assigned a $\sin x(\theta)/x(\theta)$ pattern factor. Because of the length of the array it would be desirable to calculate its radiation pattern in θ (azimuthal plane) increments of 0.005° to readily evaluate the particular thinned array being studied. However, to minimize the cost of computer time, Figs. 15-18 were calculated in θ increments of 0.1° over a θ interval of 9° and show the effects of steering the major lobe from broadside to 3.0, 5.0 and 5.006°. Figs. 19 and 20 were calculated respectively for θ increments of .005 and $.002^{\circ}$ over a θ interval of $\cong 0.2^{\circ}$ to determine the manner in which the major lobe of the array varied. This data shows that θ increments of $.005^{\circ}$ are adequate to show pattern detail and detect undesired sidelobes.

Additional data was collected for the X, K_a and E-band arrays and is summarized in Table IV. To obtain the data for Table IV radiation patterns were computed assuming no beam steer for the X and K_a band arrays for $\theta = \pm 5^{\circ}$ either side of beam maximum, in 0.0 degree increment, and for the E-band array for $\theta = \pm$ 2.5 degrees either side of beam maximum, in 0.005 degree increment. The data of Table IV is then based on approximately 1000 data points for each of the arrays. From the data of Table IV, we see the percentage of thinning array be increased as the number of array elements increase. A similar observation has

2300 0.590 0.118 0.0

0	0	0	0	0	0	0	0	0	0	0	0	0	0	0	0	0	0	0	0	0	1	0	0	0	0	0	0	0	0	0	0	0	0	0	0	0	0	0	0	0	0	0	0	0	0	0	0	0	0
0	0	0	0	0	0	0	0	0	0	0	0	0	0	0	0	0	0	0	0	0	0	0	0	0	0	0	0	0	0	0	0	0	0	0	0	0	0	0	0	1	0	0	0	0	0	0	0	0	0
0	1	0	0	0	0	0	0	0	0	0	0	0	0	0	0	0	0	0	0	0	0	0	0	0	0	0	0	0	0	1	1	0	0	0	0	0	0	0	0	0	0	0	0	0	0	0	0	0	0
0	0	0	0	0	0	0	0	0	0	0	0	1	0	0	0	0	1	0	0	0	0	0	1	0	0	0	0	1	0	0	0	0	0	0	1	0	0	0	1	1	0	0	1	1	0	1	0	0	0
0	0	0	0	0	0	0	0	0	0	0	0	1	0	0	0	0	0	0	0	0	0	1	1	1	0	0	0	1	0	0	0	0	0	0	1	0	0	1	0	1	0	0	0	0	0	0	0	0	1
0	0	1	1	0	0	0	0	0	0	0	1	0	1	0	0	0	0	0	0	0	0	0	0	0	0	0	0	0	0	0	1	0	1	0	0	0	0	0	0	0	0	0	1	0	0	0	1	0	1
0	0	0	1	0	0	0	1	0	0	0	0	0	0	0	1	1	1	0	0	0	0	0	0	1	1	1	0	0	0	0	0	0	1	0	1	1	0	0	1	1	0	1	0	0	0	0	0	0	1
1	1	0	0	0	0	0	0	0	0	1	0	0	0	0	0	0	0	1	0	0	0	0	0	1	0	0	1	0	0	0	0	0	0	1	1	1	0	0	0	0	0	0	0	0	0	0	0	0	0
1	0	0	0	0	1	0	0	0	1	0	0	1	1	0	0	0	0	1	1	1	0	1	1	0	0	0	0	0	1	1	0	0	1	0	0	0	0	0	1	1	0	0	1	0	1	0	0	1	0
0	0	1	1	1	1	0	1	1	0	0	0	0	1	0	1	1	1	0	0	0	0	0	0	0	1	0	1	1	0	0	1	0	0	1	0	0	0	0	0	0	1	1	1	0	0	0	1	1	1
0	0	0	0	1	1	1	0	0	0	0	0	1	0	1	0	0	0	0	1	1	0	0	1	1	1	1	1	1	1	1	0	1	1	0	0	1	1	0	1	1	1	0	0	1	0	0	0	0	0
1	0	0	1	0	1	0	0	0	1	1	0	0	1	0	0	0	0	0	0	0	0	1	1	1	1	0	0	0	0	0	1	0	0	0	0	1	1	1	0	0	0	1	1	0	0	0	1	1	1
1	1	0	0	0	0	1	1	1	0	1	1	1	0	1	0	0	0	0	1	1	0	0	0	1	0	0	1	1	1	1	1	1	1	1	0	0	0	1	1	1	0	0	0	0	1	0	0	1	0
0	1	1	0	0	1	1	1	1	1	0	1	1	1	0	0	1	1	1	0	1	1	1	0	0	0	0	0	0	1	0	1	0	1	1	0	1	1	1	0	0	0	0	0	0	0	1	1	1	1
0	0	0	1	1	1	1	1	1	0	1	0	0	1	1	0	0	0	1	1	1	1	1	1	0	0	0	0	0	0	1	1	0	1	1	1	1	1	1	0	0	1	1	1	0	0	0	0	1	1
1	0	0	1	0	0	1	1	1	1	0	1	1	1	1	1	1	1	1	1	0	0	0	1	1	1	1	0	0	0	0	0	1	1	1	1	1	1	1	1	1	1	1	0	0	1	0	1	0	0
0	1	1	1	1	1	1	1	1	1	1	1	1	0	0	1	1	1	0	0	0	1	0	1	1	0	0	0	0	0	1	1	1	1	0	0	0	1	1	1	0	1	1	1	1	1	1	1	1	0
0	0	0	1	0	0	1	1	1	1	1	0	1	1	0	0	1	0	0	1	0	1	0	1	1	1	1	1	1	1	0	0	0	0	1	1	1	1	1	1	1	1	1	1	1	1	1	1	1	1
0	1	1	1	1	0	1	1	0	0	1	1	1	1	0	0	0	0	0	1	1	1	0	0	0	1	0	1	1	1	1	1	1	1	1	0	0	0	1	1	1	1	1	1	1	0	1	1	0	1
1	1	1	1	1	1	1	0	0	0	0	0	1	1	0	0	0	0	0	1	1	1	1	1	1	0	0	0	1	1	1	1	1	1	1	1	0	0	0	0	0	0	1	1	1	1	1	1	1	0
1	1	1	1	1	0	0	1	1	1	1	1	1	1	1	1	1	0	0	1	1	0	0	0	0	0	1	1	1	1	1	1	1	1	1	0	0	1	1	1	1	1	1	1	1	1	1	1	1	1
1	1	1	1	1	0	1	1	1	1	1	1	0	1	1	1	1	0	1	1	1	1	1	1	1	1	0	1	1	0	0	0	1	1	1	1	1	1	1	1	1	0	1	1	1	1	0	0	0	1
1	1	1	1	1	0	0	0	0	1	1	0	0	0	0	1	1	1	1	1	1	1	1	0	1	0	0	1	1	1	1	1	1	1	1	1	1	1	1	1	1	1	1	1	1	1	1	1	1	0
0	1	1	1	1	1	1	1	1	0	0	0	0	0	1	1	1	1	1	1	1	1	1	0	1	1	1	1	1	1	1	1	1	1	1	1	1	1	1	1	0	1	1	1	1	1	1	1	1	1
0	0	0	1	0	1	1	0	0	1	1	1	1	1	1	1	1	0	0	0	0	1	1	1	1	1	0	0	1	1	0	1	1	0	1	1	1	1	1	1	1	1	1	1	1	1	1	1	1	1
1	1	1	1	1	1	1	1	1	1	1	1	1	1	1	1	1	1	1	0	1	0	1	1	0	1	0	1	1	1	1	1	1	1	1	1	1	1	1	0	1	1	1	1	1	1	0	0	0	0
1	1	1	1	1	1	1	1	1	1	1	1	1	1	1	1	1	0	0	1	1	1	0	1	0	1	1	1	1	0	0	1	1	1	1	1	1	1	1	1	1	1	0	0	1	1	1	1	0	0
0	1	1	1	1	1	1	1	1	1	0	0	0	0	0	0	1	1	1	1	1	1	1	1	1	1	1	1	0	1	1	1	0	1	1	1	1	0	1	1	0	0	1	0	0	1	1	1	1	1
1	1	1	1	0	0	1	1	1	1	1	1	1	1	1	1	1	1	1	1	1	1	1	0	0	0	1	1	0	1	1	1	1	1	1	1	1	1	1	1	1	1	1	1	1	1	1	1	1	1
1	1	1	1	1	1	1	1	1	1	1	1	0	1	1	1	1	1	1	1	0	0	0	0	1	1	0	0	1	1	1	1	1	1	1	1	1	1	1	1	1	1	1	0	1	1	1	1	1	1
1	0	1	1	1	1	1	1	0	0	1	1	1	1	1	1	1	1	1	1	1	1	1	1	0	0	1	1	1	0	0	1	1	1	1	1	1	1	0	0	0	0	1	1	1	1	1	0	1	1
1	1	1	1	0	0	0	0	1	1	1	0	1	1	1	1	1	1	0	1	1	1	0	0	1	1	1	1	1	1	1	1	1	1	1	0	1	1	1	0	0	0	0	1	1	1	1	1	1	1
1	1	1	1	1	1	1	1	1	1	1	1	1	1	1	1	1	1	0	0	1	1	1	1	1	1	1	1	1	0	0	1	1	1	1	1	1	1	0	0	1	1	1	1	0	0	1	1	1	1
1	0	1	1	1	1	1	1	1	1	0	0	0	1	0	0	0	1	1	1	1	1	1	0	1	1	1	0	0	1	1	1	1	1	1	1	1	1	1	1	1	1	1	1	0	0	1	1	1	0
0	0	1	1	1	1	0	0	0	1	1	1	1	1	1	1	1	1	1	1	1	1	1	1	1	1	0	0	0	1	1	1	0	1	1	1	1	1	1	1	1	1	0	0	0	1	1	1	0	0
1	1	1	1	1	1	1	1	1	1	0	1	1	1	0	1	1	0	0	0	1	1	1	0	1	0	1	1	1	1	1	1	1	1	1	1	1	0	1	1	1	1	1	1	1	1	0	0	1	1
1	1	1	1	1	0	0	1	1	0	1	0	1	1	1	1	1	0	1	1	1	1	1	1	1	1	0	1	0	0	0	0	0	1	1	1	1	1	1	1	1	1	1	1	1	0	0	1	1	1
1	1	0	0	0	0	1	0	0	1	1	1	1	1	1	1	1	1	1	0	0	0	0	0	0	0	1	1	0	1	1	1	1	1	1	0	0	1	0	1	1	1	1	1	0	0	1	1	1	1
1	1	1	1	1	1	0	0	0	1	1	1	1	1	1	1	1	1	1	1	1	1	1	0	0	0	1	1	1	1	1	0	0	1	1	1	1	1	0	1	0	0	1	1	1	1	1	1	0	0
0	1	1	0	0	1	1	1	1	1	1	0	1	1	1	1	1	0	1	0	0	1	1	0	1	1	1	1	0	0	0	1	1	0	0	0	1	1	1	1	1	1	1	1	0	0	1	1	1	1
1	1	1	1	1	1	1	1	1	1	0	0	1	1	1	1	0	0	0	0	0	0	0	0	0	0	0	1	1	0	0	0	1	1	0	0	1	1	0	0	1	1	0	0	1	0	0	0	1	1
0	0	1	1	1	1	1	1	1	1	1	1	1	0	1	0	1	0	0	0	1	1	0	0	1	1	1	0	0	0	1	1	1	1	0	0	0	1	0	1	1	0	1	1	1	0	0	0	1	1
1	1	0	0	0	0	0	0	0	0	0	1	1	1	1	1	0	0	1	1	1	1	1	0	1	1	1	1	0	0	1	0	1	0	0	0	0	0	1	1	0	0	1	1	0	1	1	1	0	0
0	1	1	1	1	1	1	1	0	0	1	0	0	1	0	0	0	1	1	0	1	0	1	1	0	1	1	0	1	1	0	0	0	1	1	1	1	0	0	0	0	0	0	0	1	1	1	1	1	1
1	0	0	1	1	1	0	0	1	0	0	0	0	0	1	1	1	1	1	1	1	1	0	1	0	0	1	1	0	0	0	0	0	0	0	1	0	0	0	1	0	1	1	0	0	0	0	0	1	1
1	1	1	0	0	0	1	0	0	1	0	0	0	1	0	1	0	1	1	0	0	0	0	0	0	0	1	1	1	1	0	0	0	1	1	0	0	0	1	0	0	0	0	1	1	1	1	1	1	1
1	1	0	1	0	0	0	0	0	1	1	0	0	0	0	1	1	1	1	1	1	1	1	0	1	1	1	1	1	0	0	0	1	1	1	0	0	0	1	1	0	0	0	1	0	1	0	0	0	1
0	1	0	0	0	0	1	1	1	1	0	1	1	0	0	0	0	1	0	1	1	0	0	1	1	1	0	0	0	0	0	1	0	0	0	0	0	0	0	0	0	0	0	0	0	0	0	0	0	0
0	0	0	0	0	1	0	0	0	1	1	1	0	0	0	1	0	0	1	0	0	0	0	0	0	0	0	0	0	0	0	0	0	0	1	0	1	1	1	0	0	0	0	1	1	0	1	1	1	0
0	0	0	1	0	0	0	0	1	1	1	1	0	0	1	1	0	0	0	1	1	1	0	0	0	0	0	0	1	1	0	0	0	0	0	1	0	0	0	0	0	0	0	0	1	0	1	0	0	0
0	0	0	0	0	0	0	0	1	0	0	0	0	0	0	0	0	0	0	0	0	0	0	0	0	0	0	0	0	0	0	0	0	0	1	0	0	0	0	0	0	0	0	0	0	0	0	0	0	0
1	0	0	0	1	0	0	0	1	0	1	0	1	0	0	0	0	0	0	1	0	0	0	0	0	1	0	1	0	0	0	0	0	0	0	0	0	0	0	0	1	1	0	0	1	1	0	0	0	0
0	0	0	0	0	0	1	1	0	0	0	1	0	0	0	0	0	0	0	0	0	0	0	0	1	0	0	0	0	0	0	0	0	0	0	0	0	0	0	0	0	0	1	0	0	0	0	0	0	0
0	0	0	0	0	0	1	1	0	0	0	0	0	0	0	0	0	0	0	0	0	0	0	0	0	0	0	0	0	0	0	0	0	0	0	0	0	0	0	0	1	1	0	0	0	0	0	0	0	0
0	0	0	1	1	0	1	0	0	0	0	0	0	0	0	0	0	0	0	0	0	0	0	0	0	0	0	0	0	0	0	0	0	0	0	0	0	0	0	0	0	0	0	0	0	0	0	0	0	0
0	0	0	0	0	0	0	0	0	0	0	0	0	0	0	0	0	0	0	0	0	0	0	0	0	0	0	0	0	0	0	0	0	0	0	0	0	0	0	0	0	0	1	0	0	0	0	0	0	0

TABLE III

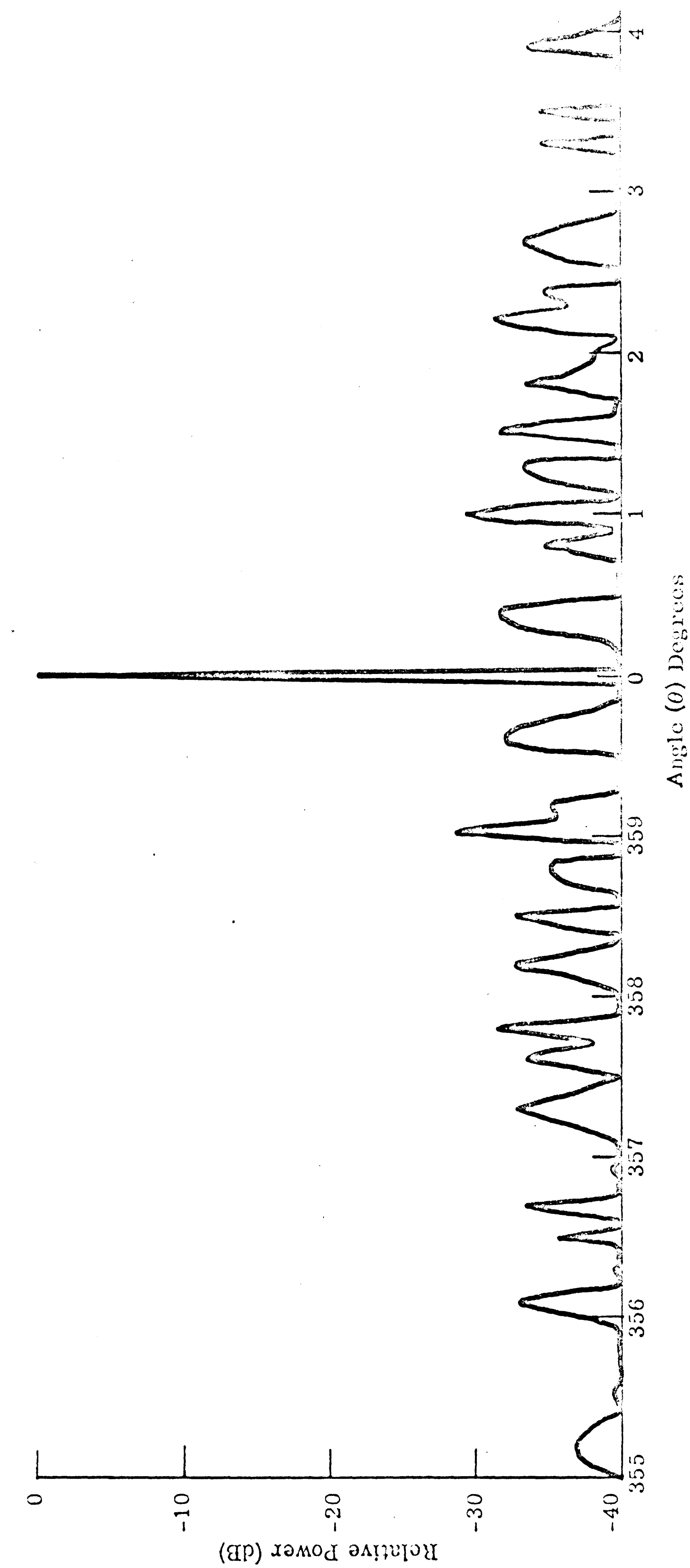

FIG. 15: Array Thinned 50 percent, Beam Steer = 0^{o}, Data Calculated in 0.1^{o} Increments.

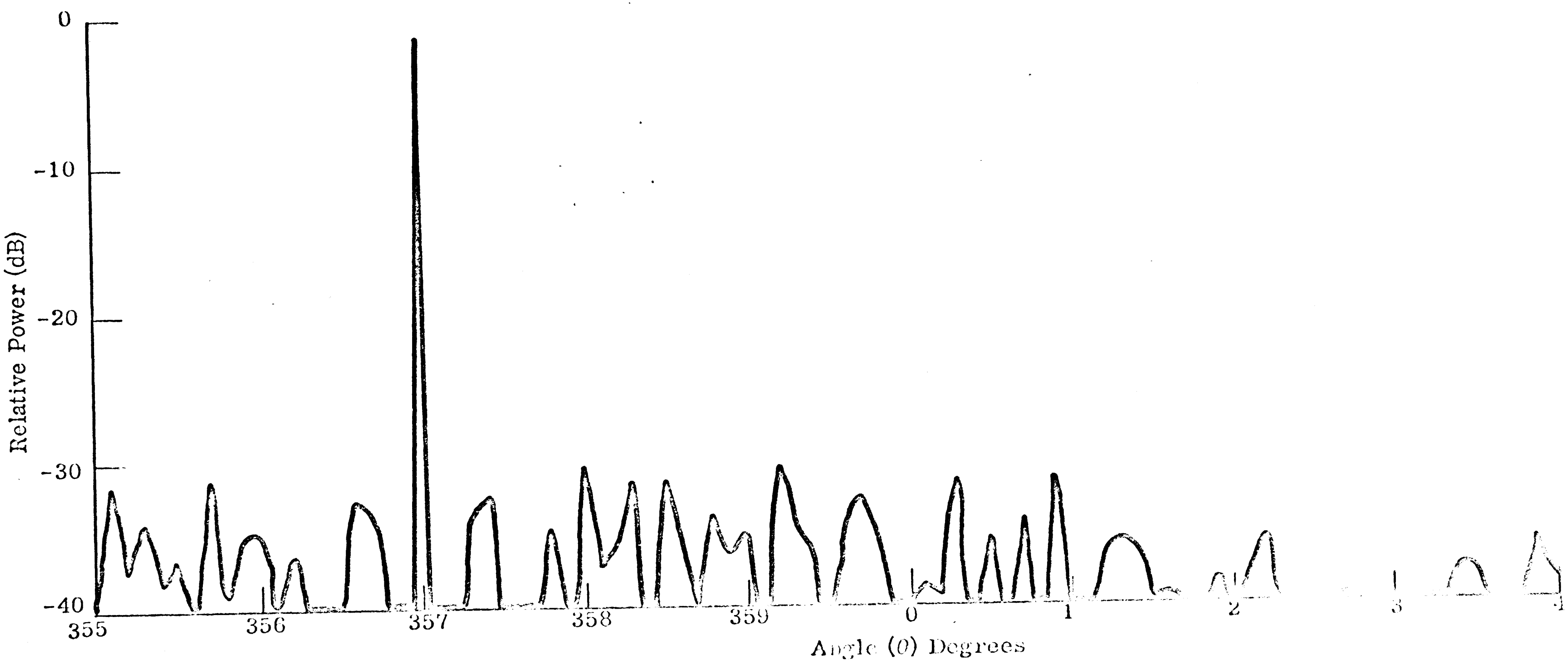

FIG. 16: Array Thinned 50 percent, Beam Steer = -3°, Data Calculated in 0.1° Increments.

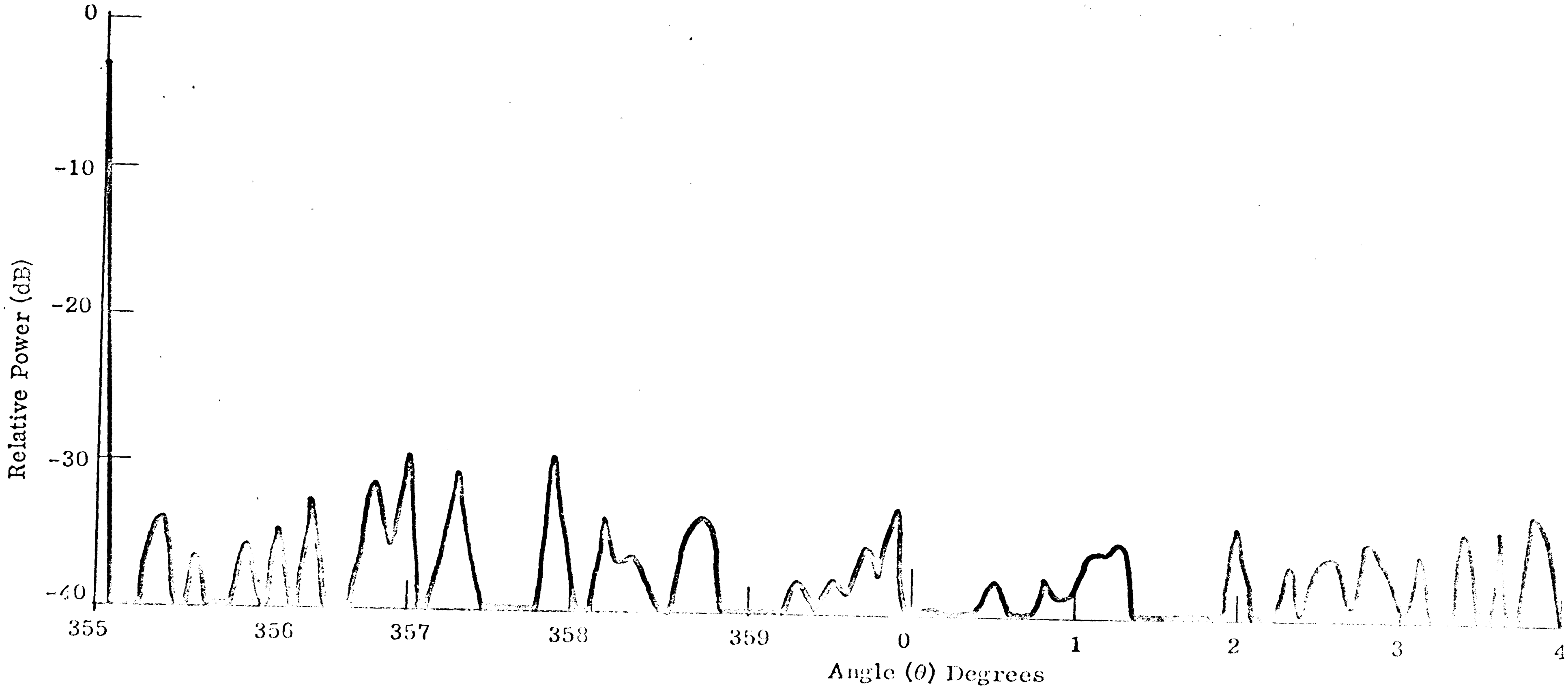

FIG. 17: Array Thinned 50 percent, Beam Steer = -3°, Data Calculated in 0.1° Increments.

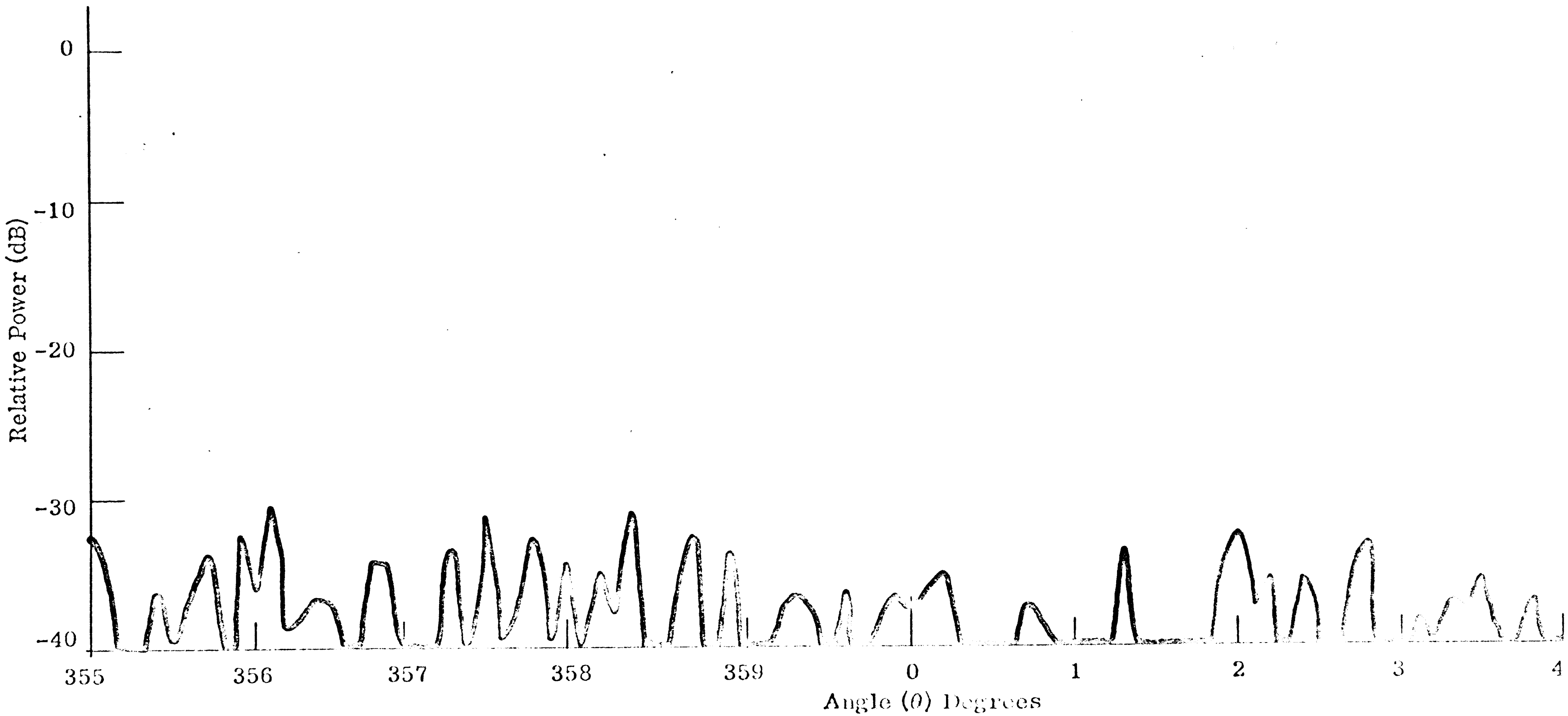

FIG. 18: Array Thinned 50 percent, Beam Steer = 5.006°, Data Calculated in 0.1° Increments.

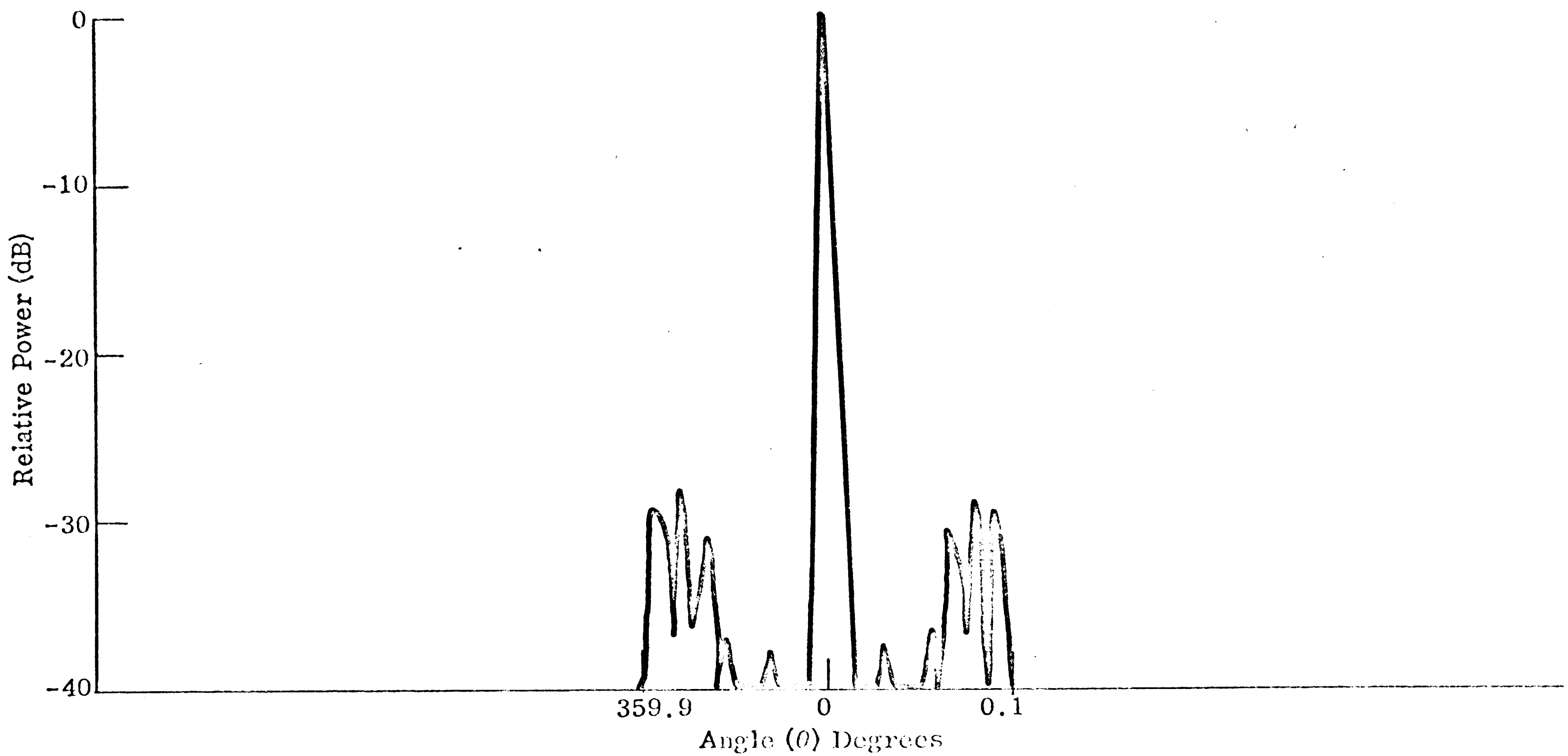

FIG. 19: Array Thinned 50 percent, Beam Steer = 0^o, Data Calculated in 0.005^o Increments.

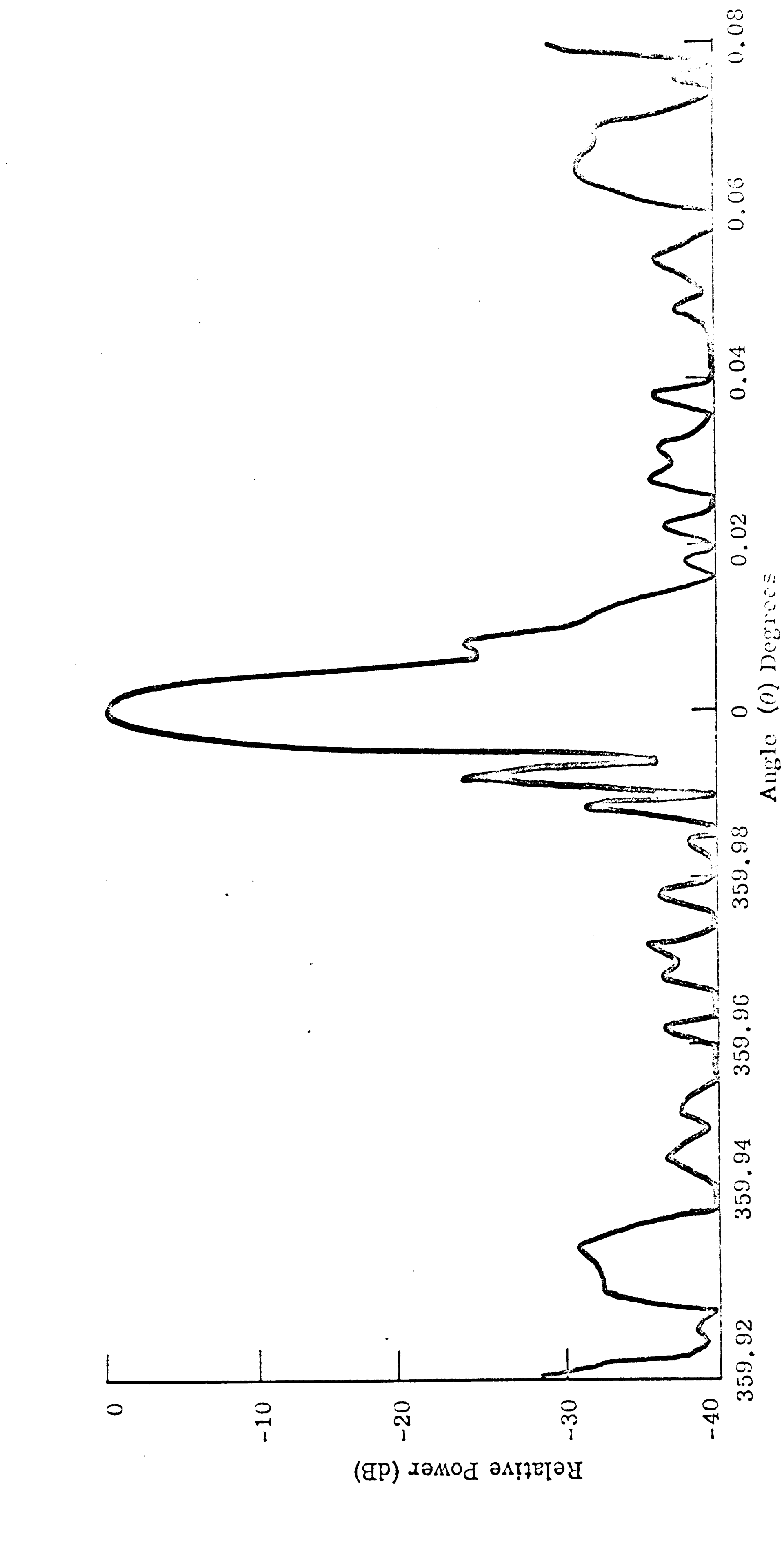

FIG. 20: Array Thinned 50 percent, Beam Steer = 0^o, Data Calculated in 0.002^o Increments.

been noted by Skolnik (op cit) and others. Specifically, the 100 foot X-band and K_a-band arrays and the 140 foot E-band array have, respectively, 200, 700 and 2800 array elements. Comparing the X, K_a-band data with the 87 percent thinned E-band data, we see that the percentage of data points - 20 dB or less (with respect to the main lobe maximum) increases from 61.8 percent for X-band to 97.6 percent for E-band.

From this exploratory study it does not appear advisable to employ a 100 foot X-band thinned array for the microwave hologram system. However, future studies associated with the development of a microwave hologram system should include a more exhaustive investigation into array thinning techniques. It is recommended that the type of computer analysis discussed here be used only in a limited way to give some direction as to the degree of thinning one may expect to achieve. However, to obtain a better insight as to the effectiveness of array thinning, or the hologram system operation, it is recommended that the array be simulated optically and tested employing optical techniques (Ingalls, 1966).

TABLE IV

Thinned Array Side Lobe Summary

(Percent Thinned)	(Percentage of Side Lobes -20 dB or less)	(Percentage of Side Lobes between -15 dB and -20 dB)	(Percentage of Side Lobes between -10 dB and -15 dB)
	10 GHz	X-Band Array (100 feet long)	
75	61.8	29.0	9.2
	35 GHz	K_a-Band Array (100 feet long)	
75	93.9	6.1	—
	9 GHz	E-Band Array (140 feet long)	
87	97.6	2.4	—
92.8	91.6	8.3	—
96.4	71.2	25.1	3.7

7.0 Side Looking-Radar Antenna Design

7.1 Antenna Configurations

The antenna recommended for the aerospace high-resolution side-looking radar system to be installed on the sky lab vehicle is a parabolic cylinder fed by a line source feed to operate at X-Band. The line source feed would consist of two edge-shunt-slot sub-arrays which would be fed from a corporate feed structure. A suggested configuration is shown in Fig. 21. This antenna is to be oriented with its long dimension (L) parallel to the vehicle's velocity vector.

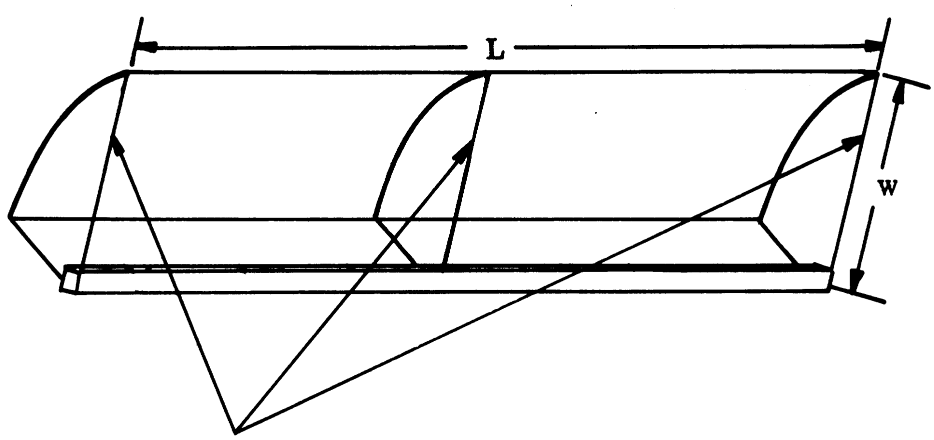

FIG. 21: Parabolic Cylinder Antenna

It is envisioned that the parabolic surface, waveguide array and necessary support truss structure be fabricated from a graphite epoxy alloy. This material is recommended because of its relatively stable thermal properties.

In Section 5.2, it was noted that the vehicle will have a finite motion, (1 degree) in roll, pitch and yaw, associated with it. Referring to the discussion of vehicle motion in Section 5.2, it is recommended that the side-looking array length be shortened to 10 feet to ensure that an adequate amount of target data is recorded in the along track direction to achieve the desired resolution.

Since the antenna is to be a parabolic cylinder fed by a line source feed, a major portion of the technical effort will be directed towards the design of the line source feed (edge-shunt-slot waveguide array).

The first question in the waveguide radiator design is whether the subsection is to be resonant or nonresonant. For the former case, a short is placed at the end of the guide, and the slots are placed at the voltage peaks, which are one-half a guide wavelength apart ($\lambda_g/2$) so the beam maximum is normal to the array. In the nonresonant design, a load replaces the short, the slot must not be $\lambda_g/2$ apart, and the beam maximum will not be at broadside. The resonant case seems more appropriate in this design because of its higher efficiency, its more desirable pattern, and the somewhat similar space taken up by the short circuit. Its drawbacks are narrower bandwidths and a need for tighter tolerances.

There are several criteria for determining the number of subsections. An array pattern analysis that includes linear FM effects is given in a previously prepared report[11]. It is shown there that center feeding is to be preferred over end feeding, and that 4 center-fed units are sufficient for satisfactory patterns. The impedance bandwidth is somewhat more restrictive. For 70 Mc total bandwidth and 20 slots per end-fed section, an input VSWR mismatch of 1.4 can be expected at the edge frequencies, compared to 1.2 with only 10 slots per section.

A usual specification is for less than $\lambda_g/4$ phase error, or a bandwidth of $50/N_s$ percent (N_s = number of slots per section), along an aperture; this specification can be met with two units. With two center-fed subsections, each of them will be 5.0 feet long. With $\lambda_g/\lambda = 1.35$ in the radiating structure and $\lambda = 0.1$ ft., the number of slots per center-fed section is

$$N_s = \frac{L_s}{\lambda_g/2} = \frac{5.0}{(1.35/2)(0.1)} \approx 72 \tag{14}$$

With a frequency change of 1/4 percent, the length of the line necessary for 36 slots with $\lambda_g/2$ spacing changes by approximately 0.0025 x 2.5 ft. or 0.00625 ft. (approximately $\lambda_g/16$). Hence for reasonable phase errors, the half-length of each unit should be no greater than 2.5 ft. On the basis of the above three considerations; (FM effects, VSWR and phase error factors), the number of units chosen is two.

7.2 Antenna Weightened Structure Assembly

The feasibility of developing a high gain intersatellite antenna (8 feet in diameter) has been investigated (Dietrich, 1970). The results of this study showed that an 8-foot diameter cassagranian antenna system could be fabricated using a graphite epoxy alloy that would weigh 27.24 pounds. This weight included the primary reflector, sub-reflector and sub-reflector strusts. Therefore, it is believed that the aerospace high-resolution side-looking antenna system would weight approximately 25 pounds. This weight includes the following components: reflector, line source feed, line source feed struts and structure truss members.

It is envisioned that the reflector would be rigidly attached to the side of the space vehicle with the line source feed folded up into the reflector during launch and until the vehicle reached orbital altitude. At the orbital altitude the feed would be released and would unfold and be positioned on the focal line of the parabolic cylinder.

The radiation patterns in the two principle planes for the subject antenna would be as follows: in the along track plane the 3 dB beamwidth will be $\simeq$ 0.6 degrees with -20 dB side lobes and in the across track plane the 3 dB beamwidth will be $\simeq$ 9.5 degrees with - 18 dB side lobes.

7.3 Environmental Problems

The pertinent environmental problems are those of micrometeorite damage, plasma sheath formation, aerodynamic drag heating, and voltage breakdown. Since no inflatable structures are contemplated, the first problem should not be severe. The second and third problems will be negligible at the design altitude assumed.

More difficult is the voltage breakdown problem. The rf voltage breakdown at X-band is most severe for altitudes near 25 n mi. In this range of altitudes, the ambient collision frequency is near the operating frequency and results in optimum breakdown conditions. Waveguide breakdown calculations indicate a permissible peak power-handling capability at these altitudes of only 9 kw for the assumed pulse length and repetition frequency. However, breakdown voltages increase rapidly as the pressure is lowered at higher altitudes. Breakdown field strengths are not tabulated for very low pressures, since breakdown then becomes independent of pressure and proportional to a constant value which is a function of waveguide surface conditions, materials, and contamination. The limit of this is well above the assumed maximum power for the system discussed in this report. Extension of the Paschen law characteristics to very low pressures indicates that ordinary rf voltage breakdown in the waveguide would not be a problem for altitudes greater than 40 n mi.

Multipactor discharges are another potential mode of waveguide breakdown. With most materials, a sufficiently energetic incident electron will cause more than one electron, also with large velocity, to leave. When this electron motion is synchronous with an rf electric field, a rapid increase in electron density is possible. This is called the multipactor or secondary electron resonance. The ultimate electron density is limited by space charge effects, but it is large enough to be considered breakdown. The results of this are severe wave attenuation and reflection.

A recent article has listed seven types of multipactor (Priest, 1963)[14]. Only three of these are pertinent to our case of an evacuated waveguide: the two-surface, the single-surface with electric field perpendicular to the surface, and the single-surface with electric field parallel to the surface. Consideration of the first order mode of two-surface multipactor indicates a power handling capability of 100 Mw. Higher order modes apparently lead to a smaller limit of power handling capability, but it appears that this limit is still greater than 10 kw. The single-surface multipactor with the electric field perpendicular to the surface should not cause trouble in the waveguide. The single-surface multipactor with the electric field parallel to the surface (primarily of concern in window failure) would not occur below a 1-Mw power level at X-band. To ensure against both rf voltage breakdown and multipactor breakdown, it is recommended that the waveguide be slightly pressurized. It would be sufficient to pressurize only that small fraction of the antenna, the feed structure, which carries sufficiently high power to make breakdown a potential hazard.

It remains to be shown that breakdown outside of the antenna cannot occur more easily than in the waveguide. Such external breakdown is a distinct possibility, since the mean free path at these high altitudes is considerably longer than the waveguide height. Breakdown outside the waveguide array may occur more readily when electrons are not lost at the metallic boundaries. However, it can be shown from the diffusion equation that the required field for breakdown when diffusion losses are absent is appreciably greater than the peak field radiated from the antenna. Thus, the possibility of breakdown would appear to be small at these high altitudes, with the specified power levels.

A final potential difficulty is changes in size of the antenna components resulting from temperature changes. Skin temperatures of a satellite vary over almost a $200^{\circ}C$ interval as a result of passage through the earth's shadow. In the event aluminum waveguides were used this would cause each subsection to change length and width (changing guide wavelength and slot spacing) with an effect on the antenna performance equivalent to changing frequency by approximately 0.48 Mc/$^{\circ}C$. The antenna temperature variation might be smaller for the present vehicle because of the vehicle size and orbit, the internal heat generation, and the possible use of a radome. With an aluminum guide and a $\pm 50^{\circ}C$ variation, the influence on pattern deterioration is the same as a $\pm$24-Mc frequency shift. The use of a graphite epoxy alloy reduces the effect to $\pm$8 Mc, which can be ignored. The entire array design must be integrated with the vehicle design to eliminate buckling, etc., so other materials might be specified in a more detailed design.

The assumption is made here that vehicle recovery is not necessary and that launch protection of the antenna can be achieved with a temporary panel to be blown off after launch. Therefore, radomes are not proposed in the present design in the interest of high efficiency and minimum weight.

7.4 Mechanical Tolerances

It has been found that fabricated arrays seldom meet theoretical design specifications because of the mechanical tolerances permitted for manufacturing purposes. The designer must either request tight manufacturing tolerances or overdesign the array (so that tolerances may be relaxed) to ensure that the electrical characteristics of the fabricated array to not deviate appreciably from those of the theoretical design. Both of these choices have disadvantages since tighter tolerances cause manufacturing costs to rise sharply, and if the array is overdesigned the antenna becomes inefficient. Since manufacturing errors mainly affect the minor lobes of the radiation pattern, the tolerances required become tighter as lower antenna sidelobes are specified. In the design of the proposed edge-slot resonant array, tolerances must be specified for the parameters of slot spacing, tilt angle, depth, and width, and for the degree to which the array may be nonplanar.

Statistical studies of the effects of mechanical tolerances on pattern deterioration have been made for a few special cases. Although not applicable per se to a particular antenna design, these studies do provide helpful guidelines. For example, O'Neill and Bailin present tolerance date for an X-band, 48-element array designed to have 20-dB sidelobes. These data show that if a tolerance corresponding to a standard deviation of 0.002 in. is permitted, 84 percent of the arrays fabricated would have 19-dB sidelobes or lower. These studies suggest that the slot parameters have tolerances of approximately $\pm 0.002\ \lambda$.

The nonplanar nature of the 20- x 1.5-foot array, which arises from bending or warping, must beconsidered. This would cause relative displacement of elements from the desired plane, which would, in turn, cause phase errors. Ruze studied errors of this type by using a correlation interval concept. Although his study was applied to reflector antennas, it should also be applicable to the distorted flat array. As a result of study by Ruze and others the usual requirement for surface tolerance for reflector antennas is $\pm\lambda/16$. In an elementary analysis of the effect of array bending on phase variations, Bailin found that a $\pm\lambda/16$ surface tolerance was also desirable for long arrays.

The standard tolerance for an X-band waveguide is $\pm$0.003 in. A uniform deviation of 0.003 in. will produce an equivalent frequency shift of 28 Mc. Since the error will be random, however, the effect will be greatly reduced and is not considered a problem.

8.0 Suggested Antenna Configurations

Here we discuss briefly the reasons for rejecting several types of antennas. Whenever possible, the superiority of a type, when restrictions are added or removed is also indicated. Reflectors, lenses, and arrays are considered, and Fig. 25 indicates each type schematically.

8.1 Reflectors

Of the five reflectors shown in Fig. 22, only the customary paraboloid type (type 1) can be rejected for a fundamental deficiency: the design aspect ratio ($D/W \simeq 20$) far exceeds the maximum feasible ratio of about 3 that can be tolerated with point feeds. The folded TEM-line feed (Schwarzschild feed) of type 2, which is often used in small ground-based radars, is much too bulky for the present application. The vertical parabolic reflectors (types 3 and 4) might have their

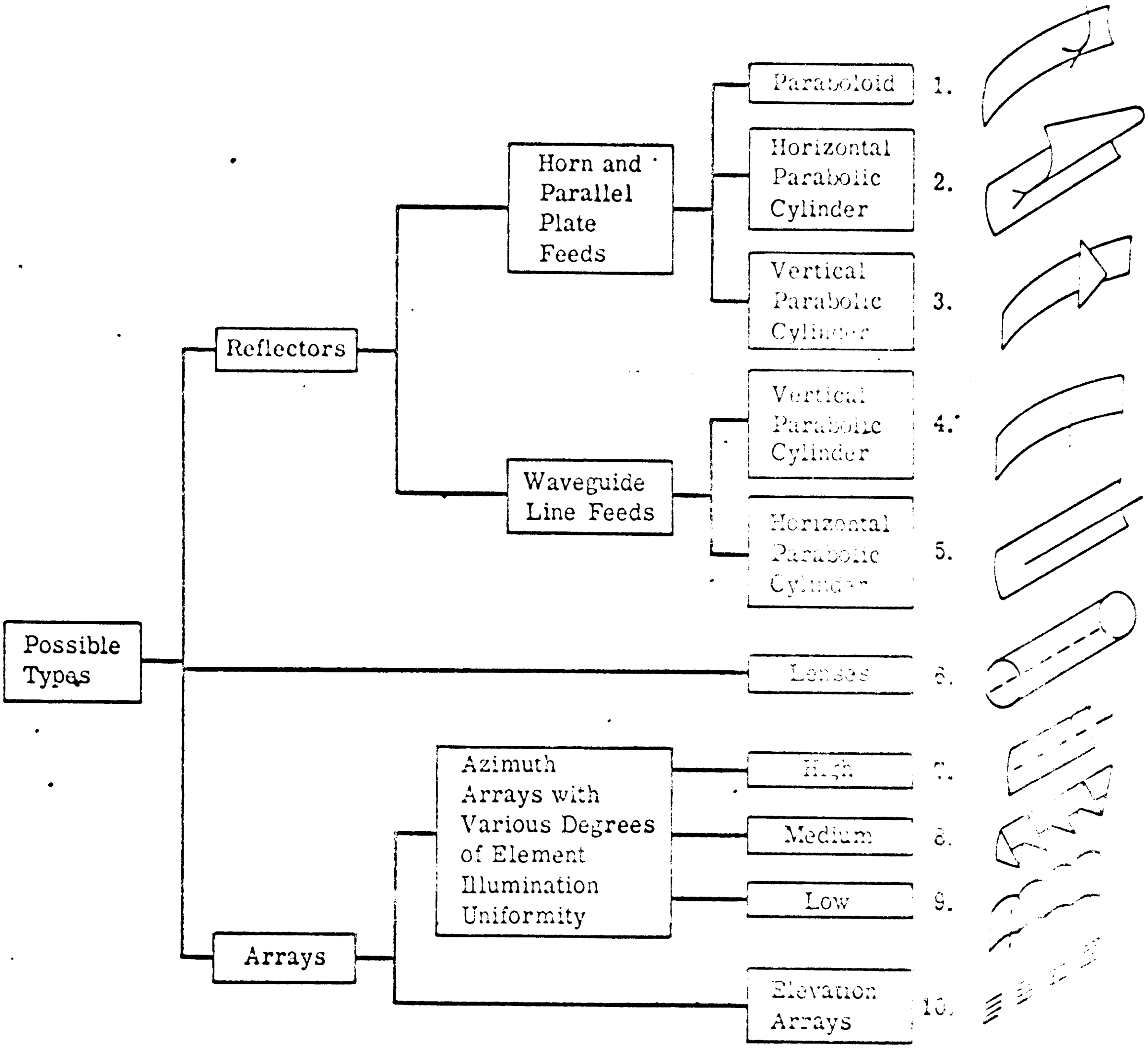

FIG. 22: Antenna Types.

greatest advantages in minimizing the weight of the antenna and the FM influence on the radiation pattern. Since they would have to be erected in space, their use might be indicated in those cases in which adequate length to house the antenna is not available, a condition not assumed in the present study. The waveguide feed with type 5, was felt to be an excellent choice to obtain a light weight antenna and relatively well controlled radiation pattern in the principal planes for the side looking antenna system.

8.2 Lenses

The lens is most often used for wide angle, relatively slow, beam steering applications. Even with multiple feeds and fast phase shifters similar to those of the waveguide array, the lens would not be preferable to the slot array because of its large required volume, greater weight, and lower efficiency.

8.3 Arrays

The azimuthal arrays in Fig. 22 (types 7-9) illustrate possible arrays of small reflectors. To satisfy the requirement of the microwave hologram array we have recommended a type 8 array. This choice was made because of the need for array thinning and the probability that this configuration (Hogg horn) would be mechanically more stable. Type 10 was rejected because of its design complexity.

References

Breakwell, J.V. and L.F. Koehler (1958), Lockheed Missile Systems Division, "Elliptical Orbit Lifetimes," 23 May 1958.

Convair (1969), "Expendable Truss Antenna Growth Characteristics," March 1969, General Dynamics Convair Division, San Diego, California, pp. 39-58.

Convair (1971), "Space and Ground-Erectable Antennas Application," August 1971, General Dynamics Convair Aerospace Division, San Diego, California.

Dietrich, F.J. (1958), "Design Consideration for High Gain Intersatellite Antenna," 1970 G-AP, IEEE Symposium, pp. 1-3.

Harger, R.O. (1970), "Synthetic Aperture Radar Systems," Academic Press.

Ingalls, A.L. (1966), "Optical Simulation of Microwave Antennas," IEEE Transactions on Antennas and Propagation, Vol. 14, No. 1, January, 1966, pp. 2-6.

Larson, R. (1971), Memo dated 24 August 1971; Subject: Initial Thoughts on Microwave Hologram -- NASA Control.

Lockheed, First Quarterly Engineering Report, (1958), 1 August - 31 October 1958, "Study and Design of Unfurlable Antennas," Vol. II, Environment and Propagation Study.

Lockheed (1970), "The Warp Rib Parabolic Reflection Antenna," 16 April 1970, Sunnyvale, California.

O'Neill, H.F. and L.J. Bailin (1952), "Further Effects of Manufacturing Tolerances on the Performance of Linear Shunt-Slot Arrays," IRE Trans. Antennas Propagation, December, Vol. 4, pp. 93-102.

Priest, D.H. (1963), "Multipactor Effects and Their Prevention in High-Power Microwave Tubes," Microwave Journal, 1963, Vol. 6, No. 10, pp. 55-60.

Ruze, J. (1952), "The Effects of Aperture Errors on the Antenna Radiation Pattern," Nuovo Cimento, 1952, Vol. 9, pp. 364-380.

Skolnik, M.I. (1969), "Antenna Theory, Part I," (R.E. Collin and F.J. Zucker), Chapter 6, McGraw-Hill Book Company.

Zimmerman, W.E. (1967), "Hologram Array Test Report," 25, July, 1967, 7016-504-M.